Perchlorate Enhances Transmission in Skeletal Muscle Excitation–Contraction Coupling

ADOM GONZÁLEZ and EDUARDO RÍOS

From the Department of Physiology, Rush University School of Medicine, Chicago, Illinois 60612

ABSTRACT The effects of the anion perchlorate (present extracellularly at 8 mM) were studied on functional skeletal muscle fibers from *Rana pipiens*, voltage-clamped in a Vaseline gap chamber. Established methods were used to monitor intramembranous charge movement and flux of Ca release from the sarcoplasmic reticulum (SR) during pulse depolarization. Saponin permeabilization of the end portions of the fiber segment (Irving, M., J. Maylie, N. L. Sizto, and W. K. Chandler. 1987. *Journal of General Physiology*. 89:1–41) substantially reduced the amount of charge moving during conventional control pulses, thus minimizing a technical error that plagued our previous studies. Perchlorate prolonged the ON time course of charge movement, especially at low and intermediate voltages. The OFFs were also made slower, the time constant increasing twofold. The hump kinetic component was exaggerated by ClO_4^- or was made to appear in fibers that did not have it in reference conditions. ClO_4^- had essentially no kinetic ON effects at high voltages (≥ 10 mV). ClO_4^- changed the voltage distribution of mobile charge. In single Boltzmann fits, the midpoint potential $\overline{V}$ was shifted -20 mV and the steepness parameter K was reduced by 4.7 mV (or 1.78-fold), but the maximum charge was unchanged ($n = 9$). Total Ca content in the SR, estimated using the method of Schneider et al. (Schneider, M. F., B. J. Simon, and G. Szucs. 1987. *Journal of Physiology*. 392:167–192) for correcting for depletion, stayed constant over tens of minutes in reference conditions but decayed in ClO_4^- at an average rate of 0.3 μmol/liter myoplasmic water per s. ClO_4^- changed the kinetics of release flux, reducing the fractional inactivation of release after the peak. ClO_4^- shifted the voltage dependence of Ca release flux. In particular, the threshold voltage for Ca release was shifted by about -20 mV, and the activation of the steady component of release flux was shifted by >20 mV in the negative direction. The shift of release activation was greater than that of mobile charge. Thus the threshold charge, defined as the minimum charge moved for eliciting a detectable Ca transient, was reduced from 6 nC/μF (0.55, $n = 7$) to 3.4 (0.53). The average of the paired differences was 2.8 (0.33, $P < 0.01$). The effects of ClO_4^- were then studied in fibers

Address reprint requests to Dr. Eduardo Ríos, Department of Physiology, Rush University School of Medicine, 1750 West Harrison St., Chicago, IL 60612.

Adom González's present address is Centro de Biofísica y Bioquímica, IVIC, Caracas, Venezuela.

J. GEN. PHYSIOL. © The Rockefeller University Press · 0022-1295/93/09/0373/49 $2.00 373
Volume 102 September 1993 373–421

in modified functional situations. Depletion of Ca in the SR, achieved by high frequency pulsing in the presence of intracellular BAPTA and EGTA, simplified but did not eliminate the effects of ClO_4^-. ON humps were not observed in the depleted fibers but the slowing effect of ClO_4^-, both in ON and OFF, was still present. The shift in $\overline{V}$ was reduced to -15 mV, the change in steepness was reduced to $\sim 15\%$, and Q_{max} was unchanged. The threshold charge was reduced by ClO_4^- regardless of depletion. In fibers inactivated by prolonged depolarization ClO_4^- did not change the kinetics of charge movement (charge 2) but changed its voltage distribution, shifting $\overline{V}$ by -14 mV ($n = 6$). The Cl channel blockers A9C, SITS, and DIDS shifted threshold depolarization for Ca release to more negative potentials, but lacked other effects of ClO_4^-. The results are evidence that ClO_4^- has a complex set of effects including: (1) a negative voltage shift that at least in part is shared with other Cl channel blockers, (2) a large increase in the steepness of the charge vs. voltage distribution, which is probably mediated by Ca^{2+} released from the SR, (3) a slowing of charge movement, and (4) an improvement in the transmission from voltage sensor to release channel, manifested in a reduction of threshold charge. Effects 3 and, of course, 4 have a specific requirement, that the interaction between sensor and release channel be functional. Two possible mechanisms are considered for effects 3 and 4: a binding to the voltage sensor that is sensitive to its functional state and a binding to the release channel that affects the voltage sensor secondarily through a mechanical link. These possibilities are further explored in the following articles in this series.

INTRODUCTION

Several inorganic anions have long been recognized as potentiators of muscle contractile function. Early with the realization that muscle force was controlled by transverse tubule (T) membrane potential (Hodgkin and Horowicz, 1960*a*) came evidence that the potentiating anions lower the mechanical threshold (voltage for minimum detectable force generation; Hodgkin and Horowicz, 1960*b*). Thus, the potentiating anions were recognized to be acting on the excitation–contraction (EC) coupling process, involving the voltage sensor in their effect. The understanding of this effect stagnated until 1983, when the laboratories of H. Lüttgau and L. Kovacs (Lüttgau, Gottschalk, Kovacs, and Fuxreiter, 1983) demonstrated that the anion perchlorate (ClO_4^-) alters the intramembranous charge movement, confirming the involvement of the voltage-sensing stages of EC coupling in the effect. This work, and many other later studies, have established ClO_4^- as the most powerful known agonist of EC coupling.

Transmission from T tubule to sarcoplasmic reticulum (SR) may take place by allosteric (mechanical) interaction between the voltage sensor (DHP receptor) and the Ca release channel (Schneider and Chandler, 1973; Chandler, Rakowski, and Schneider, 1976; Ríos, Ma, and González, 1991). When ClO_4^- is present in the aqueous medium surrounding proteins it weakens interactions among subunits and favors dissociation of protein complexes. This is often attributed to chaotropic properties of this ion (Collins and Washabaugh, 1985) but there may be other explanations. It is likely that this ability to dissociate protein complexes is involved in the EC coupling effect, and a useful working hypothesis is as follows: the proteins of

EC coupling interact mechanically and ClO_4^- requires the interaction to have its effects.

A prediction from this hypothesis is that ClO_4^- should have its dramatic effects only in the presence of the assembled EC coupling system, and not on the separated individual components. Another prediction is that ClO_4^- should not be effective on cardiac muscle, where EC coupling is effected by Ca^{2+} as a chemical transmitter rather than by mechanical interaction among proteins (e.g., Nabauer, Callewaert, Cleemann, and Morad, 1989).

We proceeded to test these predictions in two steps. In the experiments in this article we studied the effect of the anion in functional muscle fibers. In the following article we compared the effects on functional EC coupling with the effects on the proteins of EC coupling (the DHP receptor and the Ca release channel) reconstituted separately in lipid bilayers or in separate vesicular fractions, as well as its effects on the L-type Ca channel of cardiac ventricular muscle.

We are interested in ClO_4^- for additional reasons. After many studies, several aspects of the effects of ClO_4^- remain unsettled. Lüttgau et al. (1983) reported an increase in the steepness of the voltage distribution ($Q(V)$) of charge movement; this was surprising, as the steepness reports an effective valence of the moving sensor. The observation was not confirmed in the more detailed study of Csernoch, Kovacs, and Szucs (1987). The latter study added measurements of calcium transients (changes in $[Ca^{2+}]_i$) but did not estimate quantitatively fluxes of Ca release. Finally, the report of Huang (1987) showed that ClO_4^- selectively altered the hump (I_γ) component of charge movement and suggested that I_β (the early, monotonically decaying component) was not affected.

In this work we used established methods of monitoring intramembranous charge movement and flux of Ca release from the SR to study systematically the effects of ClO_4^-. We described kinetic and steady-state effects on charge movement and on both early (inactivating) and maintained components of release flux. We found that ClO_4^- changes the relationship between Ca release flux and charge movement.

Additionally, we explored the relationship between the effect of ClO_4^- and physiological states by (*a*) depleting the SR of Ca and (*b*) inactivating the voltage sensor through prolonged depolarization. Under those extreme conditions the effects of ClO_4^- are simplified in ways that are helpful for clarifying the mechanisms of action.

METHODS

All studies were carried out on cut segments of fast twitch fibers from the semitendinosus muscle of the frog *Rana pipiens*, voltage-clamped in a double Vaseline gap. The design of the chamber, and techniques for dissection, voltage clamp, and measurement of membrane currents and calcium transients have been described in detail (Brum, Ríos, and Stefani, 1988; Csernoch, Pizarro, Uribe, Rodríguez, and Ríos, 1991).

Solutions

The composition of internal and external solutions used is given in Table I. Briefly, cut fiber segments ~1 cm long were mounted under a relaxing solution (consisting of isotonic potassium glutamate with 0.1 mM EGTA and 10 mM HEPES at pH 7) in a double Vaseline gap

chamber whose central (working) pool was 530 μm long. After establishing the Vaseline seals, the continuity of the membrane in the end segments was broken by notches made with scissors, or, in all experiments with identification numbers greater than 762, by a brief exposure to a low concentration of saponin (Irving, Maylie, Sizto, and Chandler, 1987) followed by thorough washing with the relaxing solution. The internal solution, consisting mostly of Cs glutamate, was heavily buffered for Ca to avoid contraction. The Ca buffer was EGTA (in the solutions termed *8, 15, 30,* and *60 EGTA* in Table I) and Ca was added to obtain a nominal $[Ca^{2+}]$ of 20 nM (unless otherwise indicated). The amount of Ca added was calculated assuming a dissociation constant for EGTA: Ca of 4.9×10^{-7} M (in turn calculated at pH 7.0 using stability constants given by Martell and Smith [1972] and corrections for temperature and ionic strength described by Harafuji and Ogawa [1980]). We sought to use the minimum [EGTA] that prevented movement, and this was found to vary with individual frogs or batches of animals. In

TABLE I

Solutions

	Internals				Externals		
	8 EGTA	*15 EGTA*	*30 EGTA*	*60 EGTA*	*Ca*	*Ca-Co*	*Co*
Antipyrylazo III	0.8	0.8	0.8	2	—	—	—
ATP	5	5.5	6.1	5	—	—	—
Ca	*	*	*	*	10	2	—
Cl	12	11.94	16.60	12	—	20	20
Co	—	—	—	—	—	8	10
Cs	102	101	106	130	—	—	—
CH_3SO_3	—	—	—	—	130	110	110
EGTA	8	15.86	31.73	60	—	—	—
Glutamate	95	46	46	10	—	—	—
K	10	10	10	10	—	—	—
Mg	6	5.97	6.7	6	—	—	—
Na	10	30	12	10	—	—	—
Pyruvate	—	20	—	—	—	—	—
TEA	—	—	—	—	122.5	120	120

All concentrations are in millimolar.

*The internal solutions had calcium added for a nominal $[Ca^{2+}]$ of 20 nM unless stated otherwise. All internal solutions had 5 mM creatine phosphate and 5 mM glucose. All external solutions had 1 μM TTX and 1 mM 3,4 diaminopyridine. All solutions had 10 mM HEPES and were titrated to pH 7 at room temperature.

the experiments of depletion of Ca in the SR we used *60 EGTA* or solutions containing both EGTA and BAPTA and no added Ca.

The *external solutions* contained mostly TEA methanesulfonate. The three external solutions differed in the nature but not the total concentration of divalent cations. When the intention was to explore the distribution of charge in an extended voltage range, the solutions *Ca-Co* and *Co* were used. In a separate series of experiments (Pizarro, G., and E. Ríos, unpublished observations), exposure of fibers to solutions with 100 mM extracellular $[Co^{2+}]$ resulted, in ~50% of the cases, in changes in the resting spectrum of the fiber, consistent with formation of dye:Co complexes inside the cell. These changes were accompanied by reduction in the Ca^{2+}-related optical signal. For these reasons, the experiments aimed at exploring the relationship between charge and Ca release flux were carried out in *Ca* extracellular solution and were restricted to voltages below −10 mV. The osmolality of external solutions was

adjusted to 0.26 osmol/kg and that of the internal solutions to 0.25 osmol/kg (as suggested by Heiny and Jong, 1990). The pH was 7.0 and the temperature was between 10 and 14°C.

Data Acquisition

The fibers were kept at a holding potential (HP) of −90 mV. Sometimes the HP was changed to −80 or −100 mV, attempting to situate it about −30 mV from the threshold voltage for minimum detectable Ca^{2+} transients. Upon pulsing, four signals were acquired: total current, measured voltage (voltage difference between one end pool and the external pool), and transmitted light intensities at 720 and 850 nm (Brum et al., 1988). Data were conditioned by 8-pole Bessel filtering at 2 kHz and were acquired with a 12-bit conversion board (DMA 100; Scientific Solutions Inc., Solon, OH) under a 386 based PC-compatible computer (CompuAdd Corp., Austin, TX). The acquisition board sampled four channels sequentially at 100 kHz, and then averaged five contiguous samples per channel to obtain four almost synchronous averages every 200 μs. These values were stored as records of 1,280 points (256 ms). Other frequencies were used but are not shown. Digital filtering, in the form of symmetric (smoothing) routines, was used only if specified.

Calcium Measurement

The internal solution always contained the dye antipyrylazo III at 0.8 mM. The dye concentration in the working pool was monitored by the change in absorbance at 550 nm (Kovacs, Ríos, and Schneider, 1979). The time course of change in free $[Ca^{2+}]$ was derived from the changes in absorbance at 720 and 850 nm as described before (Brum et al., 1988). The records of $[Ca^{2+}](t)$ were often decimated, replacing every five successive values by one average. This reduced the time required for the fitting routines described below. All $[Ca^{2+}](t)$'s illustrated in this paper are decimated records.

Estimation of Calcium Release Fluxes

The time course of $[Ca^{2+}]$ during pulses of different duration and intensity was used to derive the time course of flux of Ca release from the SR ($\dot{R}(t)$), using the method of Melzer, Ríos, and Schneider (1984, 1987) modified as described by Brum, Ríos, and Schneider (in Brum et al., 1988, Appendix). In this method the first step is to estimate the rates of calcium removal from the myoplasmic solution. This is done using a model of removal including terms with the same formal properties as the proteins (troponin, parvalbumin), transport systems, and extrinsic Ca binding molecules added in the experiment (dye, EGTA, BAPTA if used). A computer program finds, through a nonlinear least-squares routine (Scarborough, 1968), a set of model parameters so that the decay of several Ca transients at different voltages and durations is well fit. This first step is illustrated in Fig. 1, which shows several Ca transients that were fitted simultaneously (noisy records). The smooth curves after the end of the pulses are the theoretical time courses of decay generated with the model and a best fit set of parameters. The simulated records start 15 ms after the end of the pulses as the removal model assumes that the voltage-dependent release of calcium has ended by then.

Normally the fitting routine starts from a set of values that were found to describe well the transients of the set of fibers studied by Brum et al. (1988) plus an additional binding molecule (EGTA) at the concentration of EGTA present in the end compartments, with rate constants $k_{ON\,C_a\,EGTA} = 1.5\ \mu M^{-1}s^{-1}$ and $k_{OFF\,C_a\,EGTA} = 0.5\ s^{-1}$. Initially three parameters are allowed to vary; once a convergence criterion is satisfied, the program explores other parameters, which are simultaneously varied in groups of two or three, until no further improvements are achieved. After finding a suitable set of parameters, these are used to reconstruct the release flux during a given transient. The heavy trace in Fig. 3 represents the release flux $\dot{R}(t)$ obtained from the Ca^{2+} transient at the top of Fig. 1.

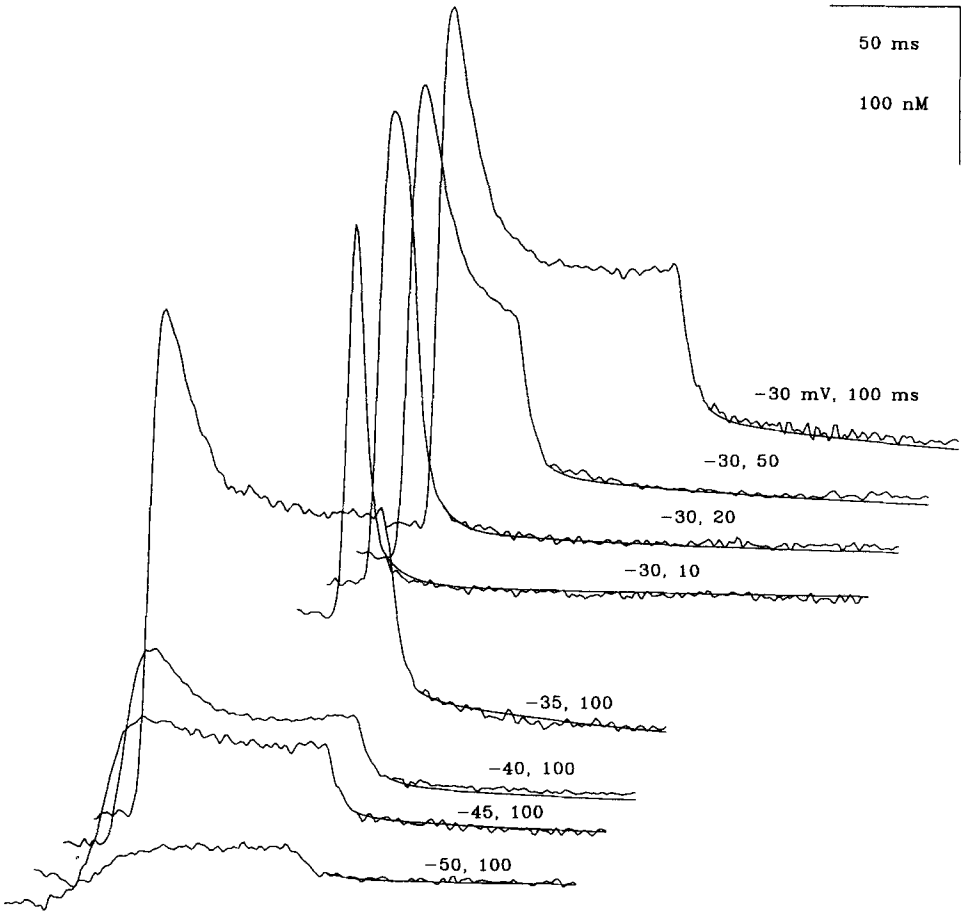

FIGURE 1. Fits of calcium removal. Shown are Ca^{2+} transients obtained with pulses of the voltage and duration indicated next to each record from a HP of −90 mV. The lower three records are averages of two and the others are single sweeps. The smooth lines start 15 ms after the end of each pulse and are simulations of the time course of $[Ca^{2+}]_i$ with the removal model described in the text and in Brum et al. (1988) and a set of parameters that give the best fit to the records shown and three other records. The parameters, their symbols, and their best fit values are as follows: rate constant of dissociation of Ca^{2+} from troponin ($k_{OFF\,C_a}$), 600 s^{-1}; $k_{ON\,C_a\,T}$, 100 $\mu M^{-1}\,s^{-1}$; rate constant of dissociation of Ca^{2+} from parvalbumin ($k_{OFF\,C_a\,P}$), 2.9 s^{-1}; $k_{ON\,C_a\,P}$, 100 $\mu M^{-1}\,s^{-1}$; $k_{OFF\,Mg\,P}$, 2.7 s^{-1}; $k_{ON\,Mg\,P}$, 0.04 $\mu M^{-1}\,s^{-1}$; maximum transport rate of the SR pump (M), 9.8 mM s^{-1}; dissociation constant of Ca^{2+} sites on the pump ($K_{D_{pump}}$), 0.3 μM; concentration of Ca^{2+} sites on the pump ([pump]), 130 μM; concentration of Ca^{2+} sites on parvalbumin ([P]), 1.8 mM; concentration of Ca^{2+} sites on troponin ([T]), 240 μM; $[Mg^{2+}]$, 900 μM; [EGTA], 30 mM; $k_{OFF\,C_a\,EGTA}$, 11 s^{-1}; $k_{ON\,C_a\,EGTA}$, 0.77 $\mu M^{-1}\,s^{-1}$. Fiber 764. External solution, *Ca*, 8 mM ClO_4^-; internal solution, *30 EGTA;* diameter, 85 μm; linear capacitance, 27 nF; concentration of antipyrylazo III ranged between 910 μM at the beginning and 1.1 mM at the end of the series, which took 29 min. Temperature, 12°C.

It has been shown that this procedure works, as it reproduces well the time dependence of a known release flux in blind simulations (Schneider, Ríos, and Melzer, 1987*a*). There are two technical issues relative to this procedure that have to be considered when addressing any pharmacological effect: one of sensitivity and one of uniqueness of the reconstructed release records.

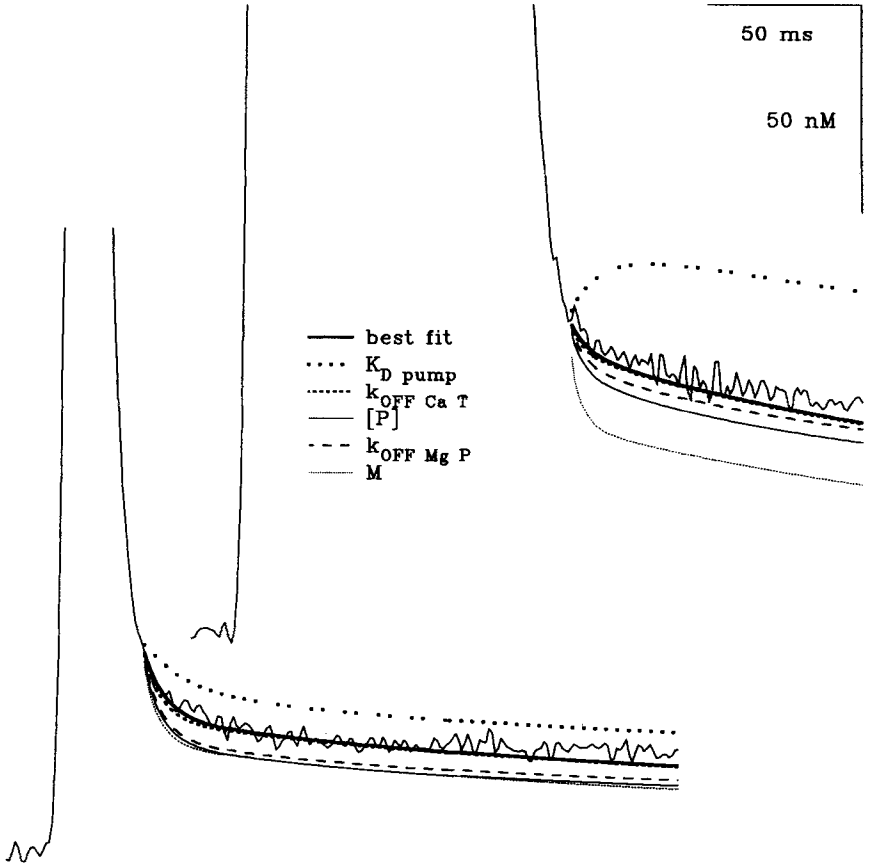

FIGURE 2. Sensitivity of the simulations to parameter changes. Thin lines represent two Ca^{2+} transients from Fig. 1 (at −30 mV, 20 and 100 ms). The thick line at OFF is the best fit with parameters listed in the legend to Fig. 1. Other lines were obtained by increasing one parameter at a time by a factor of 3. The parameters changed are keyed to the lines on the figure. The consequences of changing other parameters are described in the text.

Sensitivity of the Evaluation of Ca Removal

The release flux calculated by this method is dependent on the estimation of removal properties. If an agent like perchlorate is found to change the calcium transients, it may have changed removal, release, or both. Fitting the removal model is an obvious procedure to evaluate whether perchlorate causes changes in this function. Some results are presented later.

Fig. 2 illustrates a simulation devised to explore the sensitivity of the fitting procedure. It replots two of the Ca^{2+} transients of Fig. 1 at a much greater scale. The various smooth curves

at the OFFs are simulations obtained changing one at a time the fit parameters of Fig. 1. The change is always a multiplication by 3 of one parameter, leaving all others unchanged.

Qualitatively, the alternative simulations show that a threefold increase in either the dissociation constant of the pump (K_D), the maximum pump rate (M), the concentration of parvalbumin ([P]), or its OFF rate constant for Mg binding ($k_{OFF\,Mg\,P}$) should be easy to detect. Quantitatively, the standard error of fit increases more than twofold from its best fit value of 4 nM. Thus if ClO_4^- caused changes of this magnitude in the removal functions, a worsening of the fit would reveal it.

When the total concentration of pump binding sites (considered in rapid equilibrium with Ca^{2+}) was changed from 125 to 375 μM without changing the maximum pump rate, the standard error of fit increased to 6 nM and the agreement between records and simulations was slightly but perceptibly worsened (not shown). No visible changes were caused by threefold increases in the concentration of troponin or its OFF rate constant ($k_{OFF\,C_a\,T}$), or in the corresponding ON rate constant (not shown).

The greatest changes were caused when the kinetic parameters of EGTA or its concentration were varied. This was expected, since at tens of millimolar EGTA is by far the dominant agent of Ca^{2+} removal.

An alternative way of estimating the sensitivity of the fit to changes in parameter values is through the standard error of parameter estimates (SEE), the square root of the corresponding diagonal element of the covariance matrix of least-squares fit (Cleland, 1967; Provencher, 1976). In some cases, however, the SEE could not be calculated as the diagonal elements became negative, an indication that the parameter values were not well determined. For parameters that were well determined, like the rate constants of EGTA, or the maximum pump rate, the SEE was $< 10\%$ of the best fit value. It was generally large or undefined for the rate constants and concentration of troponin and the concentration of pump binding sites.

Estimates of Release Flux Are Robust

As found in previous work (Brum et al., 1988), different sets of parameters may give equally good fits, normally through compensating changes in two or more parameters. This is revealed in the covariance matrix by large values of the corresponding cross elements. Therefore, and as remarked before (Brum et al., 1988), the particular values selected by the fitting procedure should not be interpreted as actual physical parameters. Since the choice of removal parameters is not unique, a concern here is to what extent kinetic aspects of the release records are dependent on the particular set of parameters used.

The issue is addressed in Fig. 3. An alternative fit, of equal standard error, was obtained by the program when a threefold lower value of [EGTA] was imposed (10 mM instead of the 30 mM present in the cut ends of the fiber and used for Fig. 1). The fits are not shown as they would essentially superimpose with the best fit curves in Fig. 1. The release flux records calculated with these two very different sets of best fit parameters are shown in Fig. 3. The greater calculated flux (thick trace) corresponds to the greater [EGTA].

This figure illustrates a limitation of the method: namely, the lack of uniqueness of the release records. It also illustrates a strength of the method: when the smaller record is scaled to match peaks, the time course is found to be very similar. Even though the magnitude of the computed release waveforms depends on the parameter values, their kinetics are essentially model independent. In this sense, the method can be termed robust.

Two reasons can be given for the robustness of this calculation of release. One was previously given by Schneider et al. (1987*a*), in response to concerns of Stephenson (1987). The kinetics of the reconstructed waveform are largely model independent, provided that records of several durations and voltages are fitted. The fitted set should include records obtained with pulses as short as, and shorter than, the time to peak of release. When these records are well fitted, the

method essentially performs an interpolation in time between measured values of removal flux, and the kinetics of the release waveform are determined quite uniquely. One striking example of this virtue can be seen in this article by comparing the waveforms of Fig. 3 and those of Fig. 19 *A*, in which release records of very similar time course are derived even though the Ca^{2+} transients from which they were calculated are extremely different (Figs. 1 and 18 *A*, respectively).

An additional factor reduces the model dependence further under the present conditions. Comparing the top Ca^{2+} transient in Fig. 1 and the derived release records in Fig. 3, it can be seen that their waveforms are similar. Ríos and Pizarro (1991) have shown that to be due to the presence of high [EGTA], a buffer of relatively slow binding rate constant (Smith, Liesegang, Berger, Czierlinski, and Podolski, 1984). Specifically, the removal flux will be proportional to the Ca^{2+} transient in the limit of very high concentrations of buffer, provided that the binding

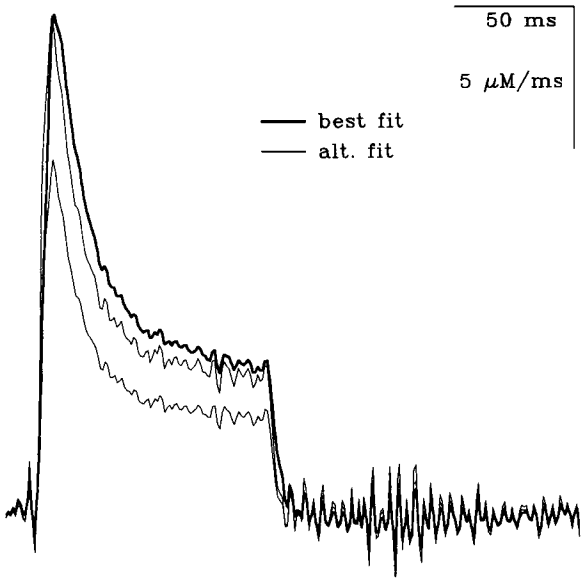

FIGURE 3. Release flux calculated with two different fits. The thick trace records the release flux waveform calculated from the Ca^{2+} transient at −30 mV, 100 ms, shown in Figs. 1 and 2 using the set of parameters listed in Fig. 1. The smallest record was obtained from the same Ca^{2+} transient and an alternative fit, of equal standard error (3.9 nM), in which [EGTA] was set to 10 mM. The larger thin trace was obtained by scaling the smaller one (by 1.4) to match the peak of the thick trace. The alternative fit had the following values: $k_{OFF\,C_aT}$, 1,600 s^{-1}; $k_{ON\,C_aT}$, 130 μM^{-1} s^{-1}; $k_{ON\,C_aP}$, 100 μM^{-1} s^{-1}; $k_{ON\,M_gP}$, 0.04 μM^{-1} s^{-1}; $k_{OFF\,C_aP}$, 4.3 s^{-1}; $k_{OFF\,M_gP}$, 1.8 s^{-1}; M, 10 mM s^{-1}; $K_{D_{pump}}$, 0.12 μM; [pump], 130 μM; [P], 1.7 mM; [T], 240 μM; [Mg^{2+}], 900 μM; [EGTA], 8 mM; $k_{ON\,C_aEGTA}$, 1.0 μM^{-1} s^{-1}; $k_{OFF\,C_aEGTA}$, 1.0 μM^{-1} s^{-1}; $k_{OFF\,C_aEGTA}$, 9.9 s^{-1}.

rate constant is slow (in the sense that the buffer is never substantially occupied). As these limiting conditions are approached, the release waveform becomes progressively better determined.

There is an advantage, therefore, in having as high a concentration of EGTA as possible. There are disadvantages: given the overwhelming influence of EGTA as an agent of removal, the improvements in fitting that can be accomplished by the program by varying other parameters of removal are quite minor and usually involve large changes in these parameters. This implies that the removal fitting procedure becomes quite insensitive to changes in the parameters (and may explain the negative covariance elements mentioned above). Therefore, the requirements for robustness and sensitivity are opposite.

Given the dominance of EGTA as the removal agent at the concentrations used, the fit depends exquisitely on its kinetic constants and concentration. We start the fitting procedure

with [EGTA] equal to the concentration in the cut ends, $k_{ON\,C_a\,EGTA} = 1.5\ M^{-1}\ s^{-1}$ (Smith et al., 1984) and $k_{OFF\,C_a\,EGTA} = 0.5\ s^{-1}$. The best fits, however, often required increasing the OFF rate constant substantially (to $\sim 5\ s^{-1}$) and better fits were often obtained with [EGTA] lower than the values at the cut fiber ends. Interactions of EGTA in the myoplasm plus large gradients of $[Ca^{2+}]_i$ along the sarcomere (Pizarro, Csernoch, Uribe, Rodríguez, and Ríos, 1991 *b*) coexisting with strongly nonlinear pumping and binding processes may all contribute to making the best fit values of kinetic constants of EGTA different from the actual concentration of EGTA and its rate constants in solution.

Having indicated the advantages of high [EGTA], we remark that the method works well in another interesting extreme situation. When a fast buffer, typically BAPTA, is present inside, simplifications are again possible (Ríos and Pizarro, 1991) and the time course $[Ca^{2+}](t)$ becomes essentially proportional to the time integral of the release flux. In this work, this situation is achieved in experiments of depletion with 1 or 3 mM BAPTA, illustrated in Figs. 18 and 19. The Ca^{2+} transients in Fig. 18 are very different from all others shown. The derived release fluxes (Fig. 19) are, however, very similar to those of Fig. 3, which is again a demonstration of the robustness of the method. As expected, the $[Ca^{2+}](t)$ waveforms are close to the time integrals of the $\dot{R}(t)$.

Measurement of Intramembranous Charge Movement

Asymmetric currents were calculated conventionally, as differences between total current during test pulses and scaled currents during control pulses of 20 mV amplitude, starting from a subtracting holding level of −140 mV unless otherwise stated. For computation of charge transfer the asymmetric current traces were corrected for sloping baselines fitted after 60 ms of ON or OFF transient and extrapolated to the beginning. Until experiment 740 the extrapolated baseline was corrected for noninstantaneous potential change as described by Chandler and Hui (1990). In those experiments we used the voltage clamp apparatus of Brum and Ríos (1987). In later experiments we adopted faster electronics, introduced by Francini and Stefani (1989), with which the potential (at the surface membrane) settles in ~0.5 ms. With this charging speed the template correction becomes unnecessary except for the very beginning of the transient. Since the rate of potential change is extremely fast during the settling time, the A/D converter frequently saturates during the first 100–200 μs of the test pulse at the gains that we find adequate for recording charge movement current (0.5 μA/V). When it was essential to record that portion accurately (when charge transfer was being measured), data were acquired at two different gains (typically 0.5 and 2.5 μA/V).

Advantages of the Saponin Procedure

There were some reproducible differences in the results obtained with the group of fibers after 762, in which saponin was used to permeabilize the cut ends, and the earlier group: (*a*) The fibers in the latter group had less electrical leak across the Vaseline seals. The leak was estimated at a HP of 0 mV from the ratio between a known potential applied to the current pool and the potential difference measured at the voltage pool. This ratio was between 80 and 95% in the early experiments. It was typically 95% in the latter group of fibers and increased to ~97% upon taking the HP to −90 mV. (*b*) There was substantially less charge movement during the control pulses in the second group. We always measure the charge movement in the control range of voltages in the manner described by Brum and Ríos (1987), that is, with a negative-going pulse to −120 mV from a prepulse level of −70 mV. We do this at the beginning of the experiments, when the fiber is held at 0 mV, and we repeat the pulse after polarization to the negative holding potential at which the experiment is carried out. The asymmetric currents recorded are illustrated for one fiber of the saponin group in Fig. 4. The

thin trace in the top record was obtained at a HP of 0 mV. The large asymmetric current is mostly charge 2 moving in the membrane of the middle portion of the fiber. In many cases there is also an excess of charge transfer during the ON due to an inward ionic current that may be eliminated with the Cl^- channel blocker anthracene 9-carboxylate (A9C). The thick trace in the top record was obtained with a similar test pulse 8 min after changing the HP to −90 mV. Unlike the fibers studied by Brum and Ríos (1987), or those studied with a

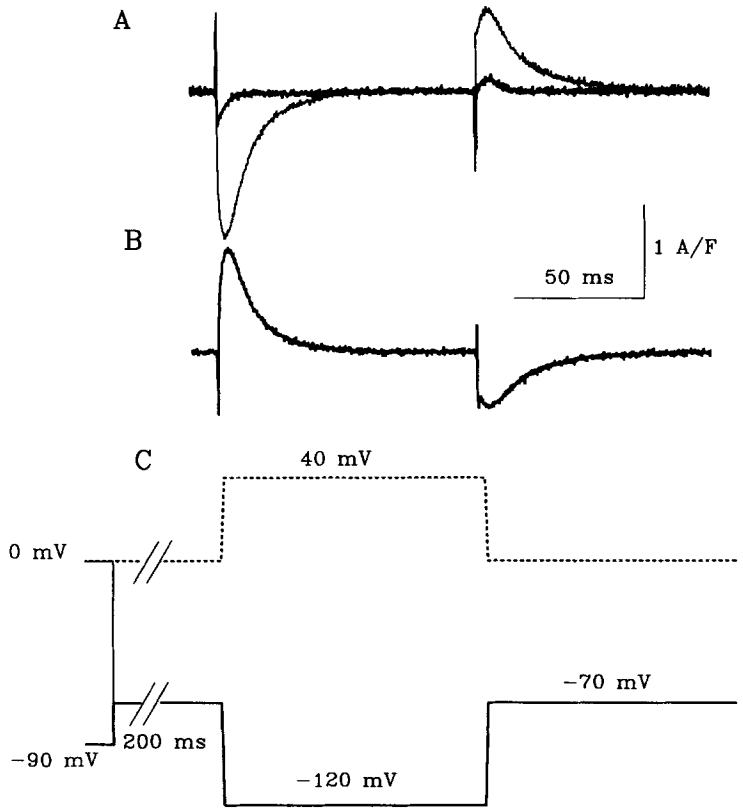

FIGURE 4. Charge in controls disappears upon negative polarization. (*A*) Asymmetric currents, calculated as the differences between currents during a test pulse from −70 to −120 mV and a control pulse from 0 to 40 mV, properly scaled to match voltages (pulses are represented schematically at the bottom). The fiber was either at a HP of 0 mV (*thick trace*) or after 8 min at −90 mV. Control currents were the same for both records. (*B*) Difference between the test currents at a HP −90 and at 0 mV. Fiber 778. External solution, *Ca;* internal solution, *15 EGTA* plus 3 mM BAPTA; diameter, 100 μm; linear capacitance, 20.6 nF; temperature, 10°C; averages of two tests and two controls.

four–Vaseline gap technique by Ríos, Pizarro, and Brum (1989), this fiber had essentially no asymmetric current in the range of charge 2 when it was held polarized. This was the case for most fibers in the group treated and all of them had at least 70% reduction in the charge measured in this way.

We could think of one explanation of this difference as a saponin effect. The charge that moves in the control range of voltages has two main sources in a polarized fiber. One is charge

2, which remains in spite of the change in HP, probably reflecting voltage sensors that remain in inactivated states (reviewed by Ríos and Pizarro, 1991). This component must have been very small in the latter group of fibers, but for reasons other than the use of saponin. Another contribution is charge 1 moving in inhomogeneously polarized regions of membrane under the Vaseline seals, where the actual voltage excursion starts more positive (Chandler and Hui, 1990). This contribution must also have been very small in the latter group of experiments. This was probably a consequence—an advantage—of the saponin permeabilization technique. Indeed, saponin is likely to permeabilize membrane up to the edge of the Vaseline seals and even under them, thus reducing the effective seal width and the area of inhomogeneously polarized membrane.

The practical consequence of this improvement is that the asymmetric currents determined in the second group of experiments are nearly free of the errors due to charge movement in the control currents. In all the experiments whose descriptions or data follow, the reduction of charge in the control range upon polarization was found to be 70% or better and remnant errors due to this cause were ignored. This was justified further by the observation that the remnant of charge in the control range usually continued to decrease for tens of minutes, beyond the level observed in the initial measurements.

For the reasons given above we now use saponin instead of notching for permeabilization of the cut ends. A large group of experiments included in this study used notching. In the description of the effects of perchlorate we include experiments with both techniques whenever possible. No systematic differences in these effects were found with the two techniques.

RESULTS

Perchlorate altered both charge movement and calcium release; it also changed the relationship between charge transferred and release flux. The results are presented in that order. Since two permeabilization procedures were used (notches and saponin) the effects are demonstrated in experiments that used both procedures.

Effects of Perchlorate on Charge Movement

ClO_4^- changes dramatically the kinetics of charge movement. Records in notched fibers are shown in Figs. 5 and 15; records from a fiber treated with saponin are shown in Fig. 13. Fig. 5 *A* shows records of asymmetric current and the corresponding records after baseline subtraction are shown in Fig. 5 *B*. 8 mM ClO_4^- (thick traces) caused many changes. The ON time course was prolonged, especially at low and intermediate voltages. The OFFs, which were roughly exponential, were also made slower, the time constants increasing in varying proportion in different experiments to between 1.5 and 5 times their reference value (typically twofold).

The most remarkable feature of the kinetic effect is the appearance of a hump at the ON, especially visible at intermediate potentials. In some cases, as in Fig. 5, there was no hump in reference and a hump appeared after ClO_4^-. In other cases (Fig. 15) a hump was already visible and ClO_4^- made it more prominent and made it appear at more negative voltages. As is clear in Figs. 5 *B* and 15, there was in many cases also an increase in the early (I_β) component.

The effect of ClO_4^- during the ON transient was practically nonexistent at higher voltages. In the experiment of Fig. 5 and in five other experiments the records at approximately +10 mV practically superimpose during the ON. Minor differences induced by ClO_4^- at the ON were not systematic. The OFF, however, was much slower

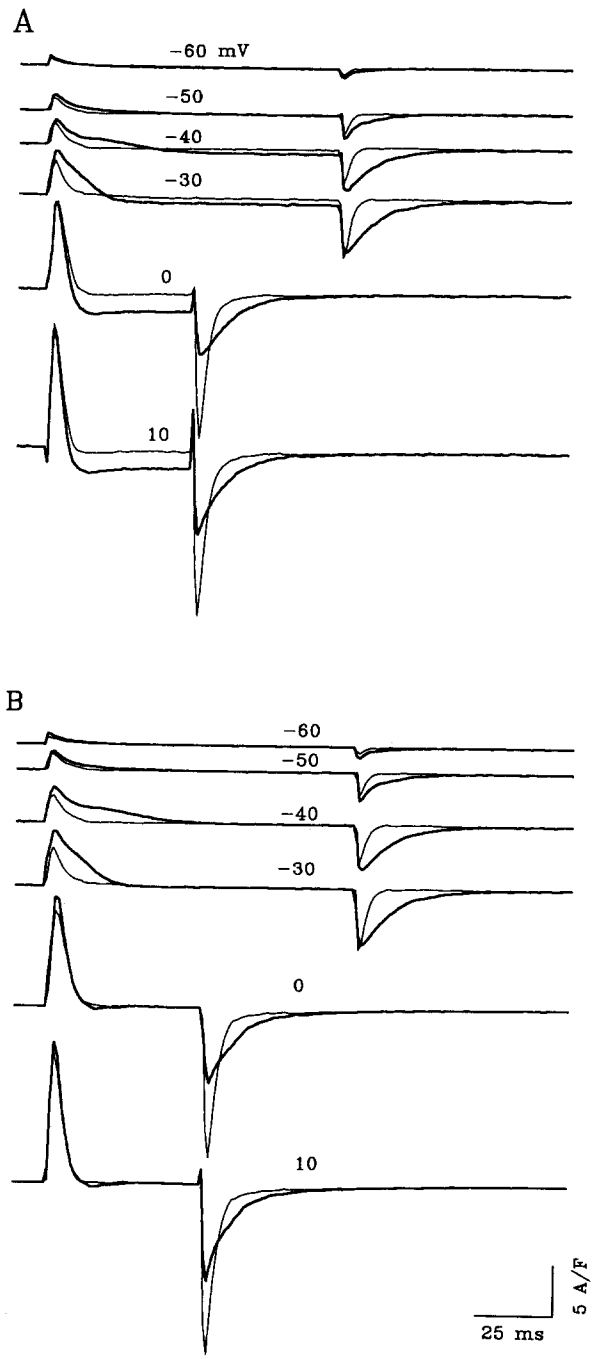

FIGURE 5. Kinetic effects of ClO_4^- on charge movement currents. (*A*) Asymmetric currents, during pulses to the voltages indicated from a HP of −80 mV. Records in the reference are represented by the thin trace. Records shown by the thick traces start after ~5 min in 8 mM ClO_4^-. (*B*) Records in *A* after subtraction of a sloping baseline fitted between 61 and 100 ms (for 100-ms duration pulses) or the average over the last 20 ms (for 50-ms pulses). Fiber 652. External solution, *Ca-Co;* internal solution, *15 EGTA*. Diameter not measured; linear capacitance, 19.7 nF. Temperature, 14°C. Averages of two tests and two controls.

in ClO_4^-, to the point that a rising phase was observable in some fibers in ClO_4^- (highest voltage in Fig. 15).

Perchlorate Induced Changes in the Voltage Distribution of Mobile Charge

The charges transferred by the current transients of Fig. 5 *B* are plotted vs. voltage in Fig. 6 in both reference (open symbols) and ClO_4^- (filled symbols). The OFF charges (triangles) became substantially greater than the corresponding ON charges above −20 mV, suggesting the activation of Ca current (even in this solution, *Ca-Co*). The curves represent Boltzmann functions fitted to ONs only. ClO_4^- at 8 mM had two effects in all nine fibers studied in this manner: it shifted the midpoint voltage $\bar{V}$ to more negative values and it increased the steepness of the best fit curve. The Boltzmann parameters are listed in Table II together with the individual differences

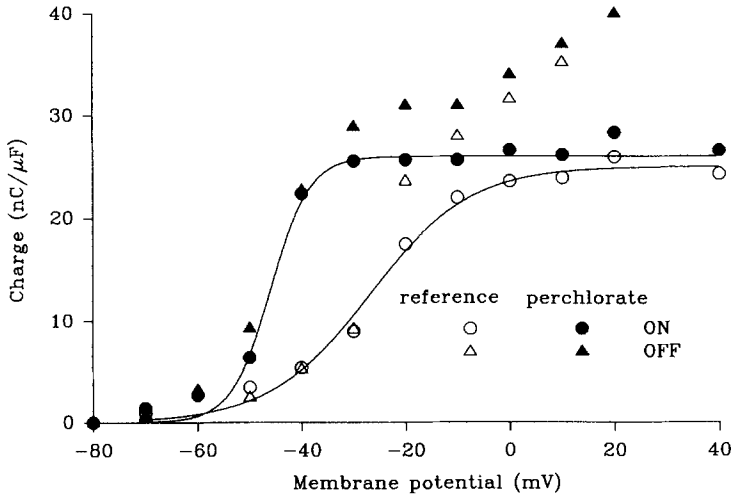

FIGURE 6. Voltage distribution of charge movement. Time integrals of the currents in Fig. 5 *B* plus other records not shown there. *Continuous lines*, single Boltzmann fits to ONs (best fit parameters in Table II). Fiber 652 (cf. Fig. 5).

induced by ClO_4^- in each fiber and their averages. $\bar{V}$ was shifted by approximately −20 mV and the steepness parameter K was reduced by 4.7 mV (the ratio of reference/perchlorate values of K was 1.77). Both effects were highly significant ($P < 0.01$) and were present in all fibers studied. The table includes two fibers (765 and 767) permeabilized with saponin. The Boltzmann parameters of these fibers do not significantly separate from the distribution defined by the other experiments.

The figure and the table also illustrate that Q_{max}, the fitted maximum of mobile charge, did not change. In summary, ClO_4^- shifted the midpoint voltage and increased the steepness of the distribution of charge. These effects strengthen the conclusion from kinetic observations that ClO_4^- increased the amount of charge moving as Q_γ. In spite of the increase in Q_γ, the total moving charge did not change. The implications of these observations will be considered in the Discussion.

Effects of Perchlorate on Calcium Removal

As a first step in the study of the effects of ClO_4^- on Ca^{2+} movements, we explored whether ClO_4^- altered removal of Ca^{2+} (following the lines described in Methods). Fig. 7 illustrates a study repeated in three fibers and shows Ca transients obtained in a saponin-treated fiber exposed to *30 EGTA* internal solution. The top group of records labeled Reference were obtained in external solution *10 Ca*. The records in the left panel were obtained in the same solution plus 8 mM ClO_4^-. Records after

TABLE II

Effect of Perchlorate on the Voltage Distribution of Charge Movement

Fiber No.	Perchlorate	Q_{max}	Differences	K	Differences	$\bar{V}$	Differences
	mM	*ηC/μF*		*mV*		*mV*	
634	0	24		8.31		−31	
	8	24	0	5.5	−2.8	−62	−31
652	0	25		9.7		−27	
	8	26	1	3.8	−5.9	−46	−19
653	0	14		9.1		−31	
	8	14	0	4.8	−4.3	−47	−16
655	0	21		10.00		−25	
	8	20	−1	5.5	−4.5	−44	−19
656	0	11		13.3		−38	
	8	10	−1	8.0	−5.3	−53	−15
657	0	11		9.7		−27	
	8	12	1	7.2	−2.5	−48	−21
685	0	25		11.0		−40	
	8	26	1	6.7	−4.3	−58	−18
765	0	21		14.1		−37	
	8	20	−1	6.2	−7.9	−51	−14
767	0	28		10.4		−36	
	8	22	−6	6.0	−4.4	−56	−19
Average			−0.7		−4.7		−19
SEM			0.7		0.5		1.8

All experiments were carried out in external solution *Ca-Co* and internal solution *15 EGTA* or *60 EGTA*. In all cases the fibers were first in reference solution and then exposed to ClO_4^-. A Boltzmann function: $Q = Q_{max}/[1 + \exp[-(V - \bar{V})/K]]$ was fitted to the charge transferred. ON values were used for fibers 652, 765, and 767 at all voltages and for voltages greater than −20 mV in all fibers; otherwise, averages of ON and OFF values were used. Fibers 765 and 767 were permeabilized with saponin and the others were notched. Averages of fit parameters, respectively, in reference and ClO_4^-: Q_{max} (nC/μF), 20 (2.1), 19 (2.0); K (mV), 10.6 (0.6), 6.0 (0.4); $\bar{V}$ (mV), −32 (1.8), −52 (2.0).

washout are also shown. The smooth curves are simulated with the removal model, fitted to the decay of $[Ca^{2+}]$ in all the records in ClO_4^- (records in the figure plus others not shown). The same parameters were then used to simulate the decay of the records in reference and washout. The fit was somewhat worse in reference (standard error increased from 6.5 to 10 nM) but was as good in ClO_4^- as after washout. Moreover, small deviations in reference and washout were in opposite directions. The overall impression is that changes in removal, if existent, were smaller than the threefold changes in pump rate simulated in Methods (Fig. 2) and that they may well

have been due to time-dependent changes in the fiber unrelated to ClO_4^-. For this reason we used the same set of parameters to reconstruct the release flux in both the presence and absence of ClO_4^-. Another possibility is that ClO_4^- changed multiple removal properties in compensating ways that still preserved a good fit with reference parameters. As discussed in Methods (Fig. 2), in that case the computed release fluxes would have a scaling error but their time course would still be well determined.

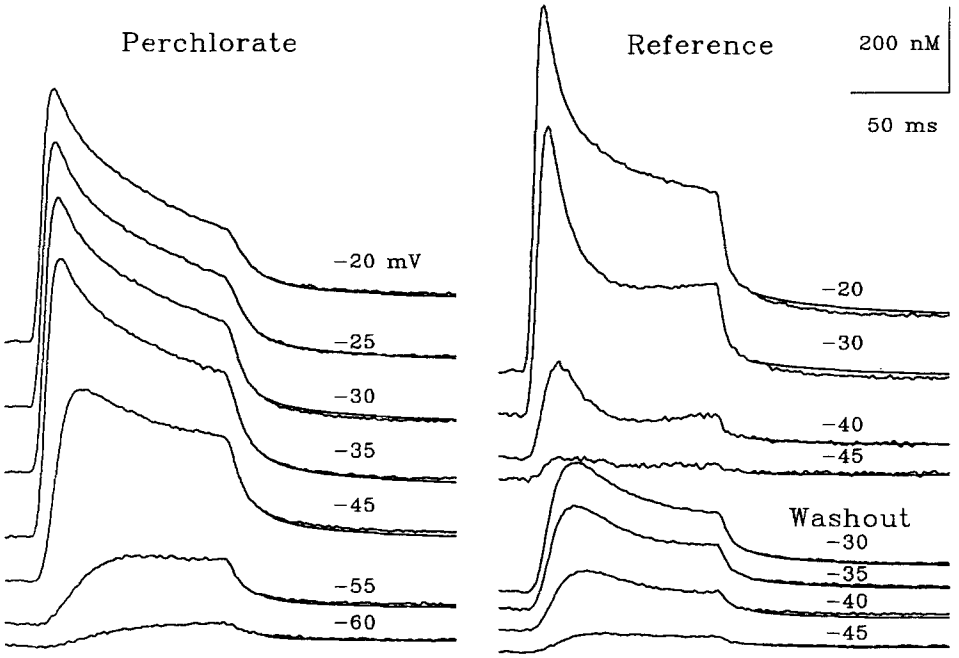

FIGURE 7. Removal fits with and without ClO_4^-. (*Left*) Ca^{2+} transients obtained in the presence of 8 mM ClO_4^-, with 100-ms pulses from −90 mV to the voltages indicated. Smooth lines are the best fits to the OFFs of these and six other records not shown, using the removal model described in Methods. The same values of the parameters were then used to simulate the OFFs of records obtained earlier in the reference solution (*Ca*) and records obtained after washout of ClO_4^- with the same solution. Parameters of removal: $k_{OFF\,C_a\,T}$, 1,200 s^{-1}; $k_{ON\,C_a\,T}$, 130 $\mu M^{-1}\,s^{-1}$; $k_{OFF\,C_a\,P}$, 1.5 s^{-1}; $k_{ON\,C_a\,P}$, 100 $\mu M^{-1}s^{-1}$; $k_{OFF\,M_g\,P}$, 5.2 s^{-1}; $k_{ON\,M_g\,P}$, 0.03 $\mu M^{-1}\,s^{-1}$; M, 9.3 mM s^{-1}; $K_{D_{pump}}$, 0.3 μM; [P], 1.0 mM; [T], 120 μM; [Mg^{2+}], 900 μM; [EGTA], 20 mM; $k_{ON\,C_a\,EGTA}$, 0.4 $\mu M^{-1}\,s^{-1}$; $k_{OFF\,C_a\,EGTA}$, 5.0 s^{-1}. Fiber 767. External solution, *Ca;* internal solution, *30 EGTA;* diameter, 83 μm; linear capacitance, 18.4 nF; concentration of antipyrylazo III ranged between 440 μM at the beginning and 950 μM at the end of the series, which took 54 min to complete. The timing aspects of the solution changes are shown in the next figure. Temperature, 10°C.

Effects of Perchlorate on Calcium Release

As observed for Fig. 3, the Ca^{2+} transients in Fig. 7 already have the shape of release waveforms and the effects of ClO_4^- can be seen qualitatively in the Ca^{2+} transients. The most obvious effect was a large reduction in the voltage for minimum detectable release.

Computed release fluxes for the same experiment are plotted in the thin traces in Fig. 8 (*A–C*). After the usual early peak, the records show a fast decay and then a noticeable second phase of decay, especially marked in the records in ClO_4^-. In some cases (Fig. 8 *B*) the two phases of decay meld in a single, quasi-exponential phase. All records shown in Fig. 8 are relatively large. Records at lower potentials had only the

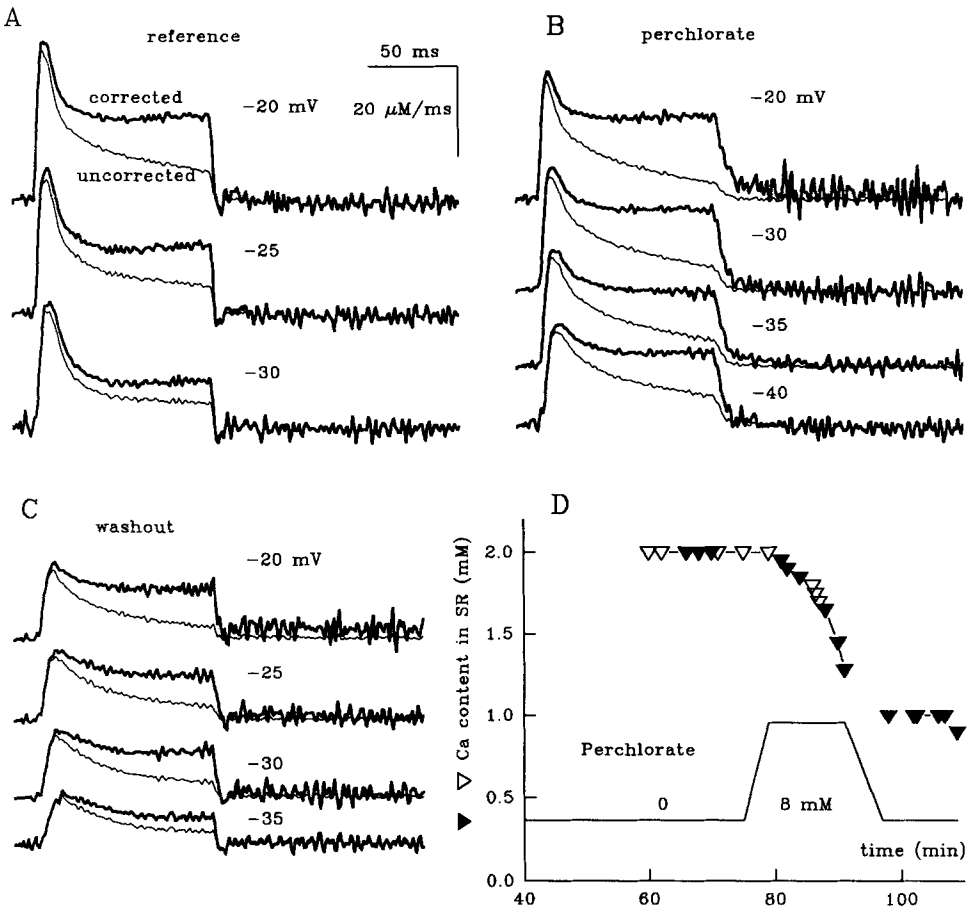

FIGURE 8. Ca^{2+} release flux and correction for depletion. Continuation of the analysis illustrated in the previous figure. The thin lines in *A–C* represent release flux waveforms computed from Ca^{2+} transients obtained in reference, in ClO_4^-, and after washout, using the removal fit parameters listed in Fig. 7. Only the large release records in each solution are shown. The thick traces were obtained from the corresponding records of release flux using the correction equation (Eq. 1) explained in the text. The single parameter Ca_{SR} was chosen to make the last 25 ms in the ON of the corrected records constant (judged by eye). (*D*) Evolution of the parameter Ca_{SR} in the successive records. Filled symbols represent values of Ca_{SR} actually fitted. Open symbols represent values extra- or interpolated from the fitted values and used to correct smaller release records (shown in Fig. 9). The plot at the bottom represents the timing of the solution changes.

fast decay, leading to a stable or slowly increasing phase (e.g., record at −40 mV in reference, Fig. 9).

The observation of a slow phase of decay after ~50 ms has been interpreted to be due to depletion of Ca^{2+} in the SR in the presence of essentially constant permeability of the release pathway (Schneider, Simon, and Szücs, 1987*b*). This view is supported by the possibility of generating records of simpler shape by the correction procedure developed by these authors and illustrated in Fig. 8. The records in the thick traces ($\dot{R}_c(t)$) were generated from the corresponding $\dot{R}(t)$ by the formula

$$\dot{R}_c(t) = \dot{R}(t) \frac{Ca_{SR}}{Ca_{SR} - \int_{t_0}^{t} \dot{R}(\tau)\, d\tau} \tag{1}$$

where Ca_{SR} is a constant representing the initial Ca content in the SR (expressed as a concentration in the accessible myoplasmic water) and the denominator is the (time-dependent) Ca content of the SR. Thus $\dot{R}_c(t)$ is the value that the release flux would have, had the SR Ca content remained constant (and assuming that the flux is proportional to the SR Ca content). $\dot{R}_c(t)$ is thus flux normalized by SR Ca content, and it has the time course of the permeability of the release pathway. In turn the value of Ca_{SR} is found by fitting the corrected release to a constant during the last 25 ms of the pulse (as shown by the records in thick trace). Therefore, the correction procedure depends on the assumption that the permeability becomes constant by ~75 ms into the pulse, and may be considered as a nonlinear fit of one parameter (Ca_{SR}).

Ca_{SR} may be different for each record, but should not change too rapidly between successive records. When pulse voltages are low, release fluxes are small and do not cause sizable depletion. In those small records (some of which are shown in Fig. 9) the correction has only a minor effect. In those cases it is not possible to fit the parameter Ca_{SR} and its value is set by interpolation between neighboring fitted values. The values of Ca_{SR} obtained from the records shown (and others) are plotted in Fig. 8 *D* as a function of time in the experiment, with surprising results. The filled triangles represent values fitted, and the open triangles represent inter- or extrapolated values.

Fig. 8 *D* indicates that the SR content diminished rapidly in ClO_4^- while remaining stable in reference and after washout of ClO_4^-. This was an unexpected recent finding in experiments that were not designed to explore this phenomenon. An evaluation of the time course of Ca_{SR} in both reference and ClO_4^- was possible in seven other experiments listed in Table III. In most it was possible to evaluate Ca_{SR} at least two times in either or both solutions. The table thus lists Ca_{SR} values and the elapsed time between both estimations. The columns *4* and *8* give the rates of change (in micromolar per second). In the fibers studied in reference, the change was essentially nil (the SR Ca content appears stable over tens of minutes). In two experiments we monitored Ca_{SR} in reference with the same pulse, repeated at low frequency for over 1 h, and found essentially no change. Of six fibers in 8 mM ClO_4^-, Ca_{SR} underwent little change in two and decayed in four. The difference in rates of change between the two conditions (differences between individual values in columns *8* and *4*) averaged −0.40 μM/s (SEM 0.18), which is significant ($P < 0.05$) in a single-sided *t*

test. Tentatively we conclude that Ca in the SR is depleted more rapidly in the presence of ClO_4^-. This may be due to increased release during the pulses or to increased release at rest.

The corrected release records $\dot{R}_c(t)$ are shown in Fig. 9. The most obvious effect of ClO_4^- is the shift in voltage for minimum detectable release, which went from −45 mV in reference to −65 mV in ClO_4^-. The maximum, $\dot{R}_p$, and the minimum, $\dot{R}_m$ (which is often the same as the steady value $\dot{R}_s$ at the end of the pulse), are plotted in Fig. 10 as a function of pulse voltage. The large symbols represent the values in reference (open circles), ClO_4^- (filled circles), and washout (triangles). ClO_4^- shifts $\dot{R}_p(V)$ by about −15

TABLE III

SR Ca^2 Content in Reference and Perchlorate

Fiber No.	1	2	3	4	5	6	7	8
	Reference				ClO_4-			
	Initial	Final	Lapse	Rate	Initial	Final	Lapse	Rate
	mM	*mM*	*min*	*μM/s*	*mM*	*mM*	*min*	*μM/s*
689	0.9	0.9	15	0.0	0.9	0.9	21	0.0
692	1.5	1.8	33	0.2	1.8	2.0	31	0.1
709	3.0	3.0	40	0.0	3.0	2.8	12	−0.3
712	‡	‡	0	‡	1.6	0.8	60	−0.2
764	0.7	1.0	20	0.3	1.4	0.7	45	−0.3
767	1.0	1.0	15	0.0	2.0	1.0	17	−1.0
774	4.0	3.9	40	0.0	*	*	17	*
1,060	3.3	3.5	75	0.0	‡	‡	0	‡
1,061	3.0	3.0	120	0.0	‡	‡	0	‡
Average				0.06				−0.28
SEM				0.04				0.15

Fibers 1,060 nd 1,061 were in external *Ca*, internal *15 EGTA* and were not exposed to ClO_4-; their diameters were 153 and 113 μm. In 1,060 the [antipyrylazo III] went from 0.36 to 0.90 mM during the lapse, and in 1,061 it went from 0.19 to 1.7 mM. The temperature was 12°C in both. All other experiments are described elsewhere. The external solution with ClO_4- was applied either before or after reference solution. In all cases [ClO_4-] was 8 mM. Columns *4* and *8* are the ratios of the increments in Ca_{SR} and the time lapses in reference (*4*) and ClO_4- (*8*). The average of column *4* is not significantly different from 0. That of column *8* is marginally significanlty less than 0 ($0.06 > P > 0.05$; one-sided *t* test). The differences (column *8* − column 4) average −0.40 (SEM 0.18, $P < 0.05$; one-sided *t* test).

*Ca_{SR} could not be determined in ClO_4-.

‡Fibers were not exposed to this solution.

mV, with a reduction in the maximum attained at high voltages. It shifts $\dot{R}_m(V)$ by some −20 mV.

Note that the values of release flux plotted by large symbols have been obtained from corrected records. This implies that the values of $\dot{R}_p$ and $\dot{R}_m$ for the same pulse are representative of the corresponding maximum and minimum of the permeabilities. Comparisons between different voltages are not so meaningful, as the Ca contents in the SR were varying rapidly while in ClO_4^-. The figure also shows sets of smaller symbols for the data in ClO_4^- and washout. These plot the values

$$\dot{R}_p(V)^* = \dot{R}_p(V) \times 2\ \text{mM}/Ca_{SR}$$

and

$$\dot{R}_m(V)^* = \dot{R}_m(V) \times 2 \text{ mM}/Ca_{SR} \quad (2)$$

2 mM is the value of Ca_{SR} in the initial run in reference. The small symbols thus represent release flux at a constant initial content of 2 mM and express the voltage dependence of the maximum and minimum permeability of the release pathway. Two outcomes of this analysis are that the fiber was stable in terms of gating

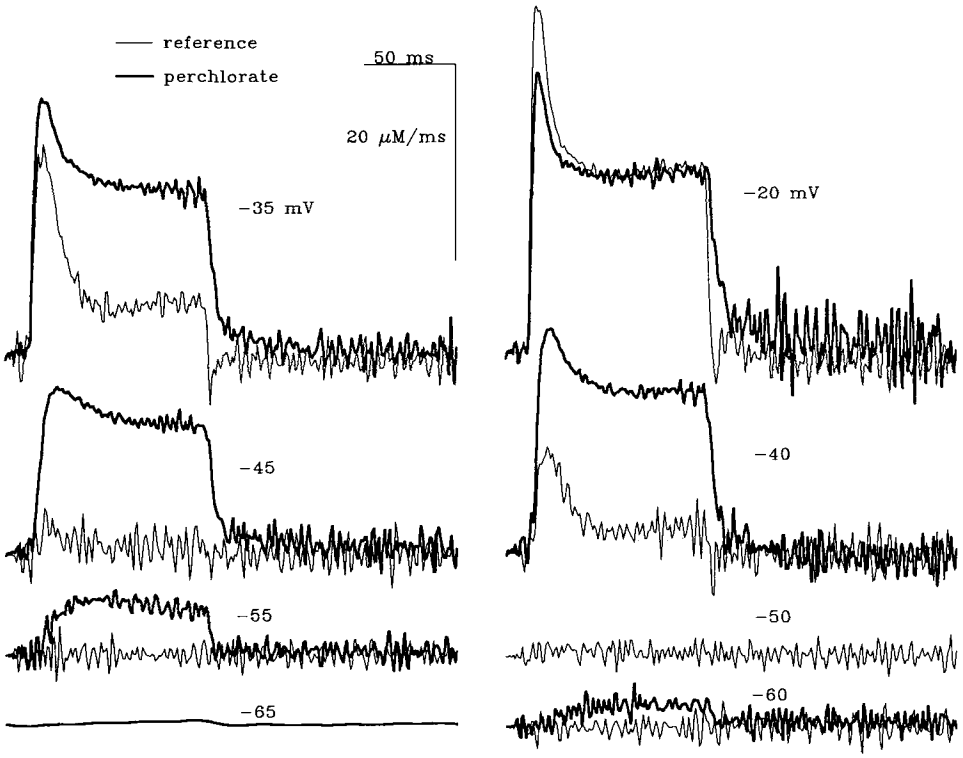

FIGURE 9. Effects of ClO_4^- on release flux. Representative release fluxes from the experiment illustrated in the previous figures are shown, corrected for depletion and superimposed to show the effects of ClO_4^- (the records at −40 mV and above in ClO_4^- and at −30 mV in reference were already shown in Fig. 8). The record at −65 mV in ClO_4^- is shown after a 20-ms smoothing procedure to demonstrate the activation of release at this voltage. Heavily filtered versions of other records in this group are shown in Fig. 11.

properties (as shown by the superposition of $\dot{R}_p^*$ in reference and washout) and that the effects of ClO_4^- were fully reversible. Another observation is that the washout values of $\dot{R}_m^*$ stay higher than reference, consistent with the usual attenuation of inactivation of release that is found in the course of a long experiment, regardless of the treatment. According to this analysis, the permeability (both peak and minimum) still increased with voltage at −20 mV in this fiber.

Perchlorate Changed the Proportion of Inactivating Release Flux

ClO_4^- changed the kinetics of release, as shown in Fig. 9. In ClO_4^-, the pulses in the just suprathreshold range of voltages elicited monotonically increasing releases rather than the habitual inactivating waveform. The effect is illustrated with two of the smaller records of Fig. 9, which are replotted in Fig. 11 after digital filtering. The records at −60 mV in ClO_4^- and at −45 mV in reference were chosen because they reach about the same maximum value and presumably similar levels of local $[Ca^{2+}]$,

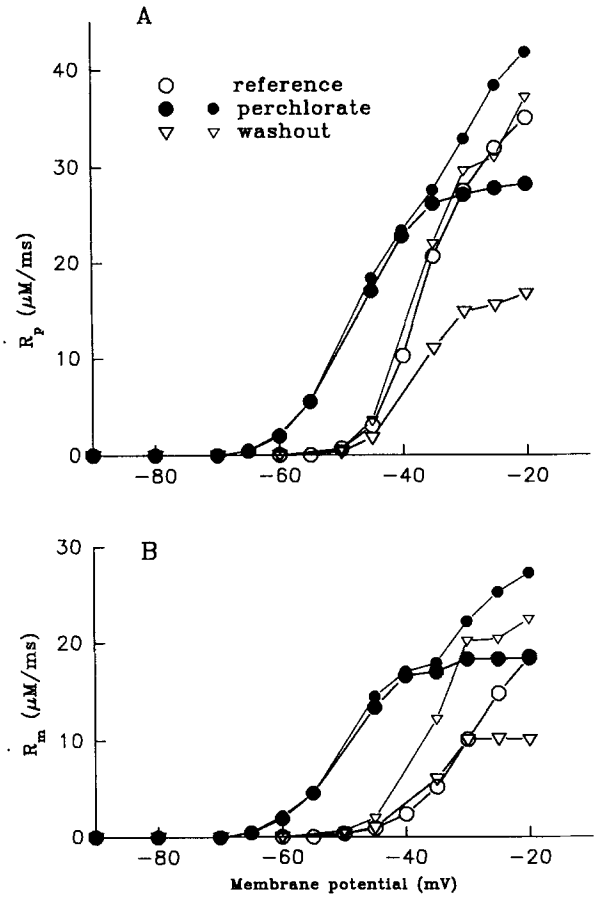

FIGURE 10. Voltage dependence of maxima and minima of release flux. $\dot{R}_p(V)$ (*A*) and $\dot{R}_m(V)$ (*B*) are derived from the records in Fig. 9 (and others) by averaging the values of $\dot{R}(t)$ for 2 ms around the maximum (for $\dot{R}_p$) and 10 ms around the minimum or 10 ms at the end of the pulse when there was no local minimum (for $\dot{R}_m$). The small symbols plot values of $\dot{R}_m^*$ and $\dot{R}_p^*$ obtained from the above by Eq. 2.

which makes it unlikely that the differences in inactivation are due to different local concentrations. Also plotted is the release at −45 mV after washout, which displays, attenuated, the characteristic inactivating shape of the reference record. The records in Fig. 11 *B* are from a different fiber, permeabilized by notches (709), and show similar effects. This experiment is illustrated in detail later (Figs. 15–17).

Not only did ClO_4^- extend the region of voltages that elicited monotonic release waveforms, it generally reduced the proportion of inactivating release flux over most

of the voltage range. The relative importance of the two components of the release waveform is conveniently represented by the fractional inactivation (F_i),

$$F_i \equiv (\dot{R}_p - \dot{R}_m)/\dot{R}_p$$

calculated in all cases after correction for depletion. Its voltage dependence in both experiments of Fig. 11 is represented in Fig. 12. In the saponin-treated fiber in reference condition (open circles) F_i went through a maximum at −40 mV and then decayed throughout the voltage range. (In other fibers in reference solution F_i went through a maximum at a slightly suprathreshold voltage and then decayed and

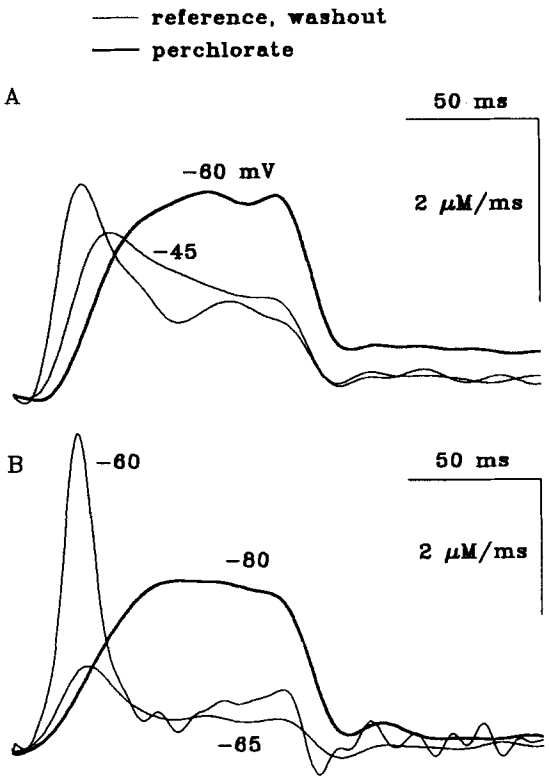

FIGURE 11. Perchlorate alters kinetics of release. (*A*) Selected $\dot{R}_c(t)$ records from the experiment in the preceding figures, digitally filtered (20-ms smoothing). The faster record shown by thin trace is in the reference and the other is after washout. The records in ClO_4^- and reference were shown in the previous figure without filtering. (*B*) Smoothed records of release flux from a different fiber, permeabilized by notching (709, described in detail in Figs. 15–17). The fiber was held at −100 mV and pulsed for 100 ms to the voltages indicated.

stabilized at a lower value at high voltages.) In ClO_4^- (filled circles) F_i was zero at −65 and −60 mV (the waveform of release was monotonic; Fig. 9) and then increased without reaching a peak and without reaching the values of F_i in reference. After washout (triangles) inactivation regained the local maximum although F_i stayed well below reference values. In the notched fiber (squares) ClO_4^- eliminated the local maximum of $F_i(V)$. In all fibers studied the effect was similar, ClO_4^- reduced or eliminated the local maximum of $F_i(V)$, but in some the F_i in ClO_4^- reached reference values at high voltages (not shown).

Perchlorate Reduced Threshold Charge

It was shown in Fig. 10 that $\dot{R}_m(V)$ was shifted by about −20 mV in ClO_4^-. In general this shift was −20 to −30 mV and was greater than the shift in $Q(V)$ (Table II). Given this difference, it was expected that Q_{th}, the charge transfer for minimum detectable release, would decrease in ClO_4^-, and this was found to be the case. This is an issue of theoretical importance, as it implies that the anion does not simply affect the voltage sensor, but also its interactions in the coupling process. The key observations will be illustrated for the same saponin-treated fiber of the previous figures (767) and for one notched fiber (709).

Slightly suprathreshold charge movement records from the saponin-treated fiber are shown in Fig. 13. The records in reference and perchlorate are obtained at intervals of 5 mV, starting with the voltage that gave the smallest hint of release. The

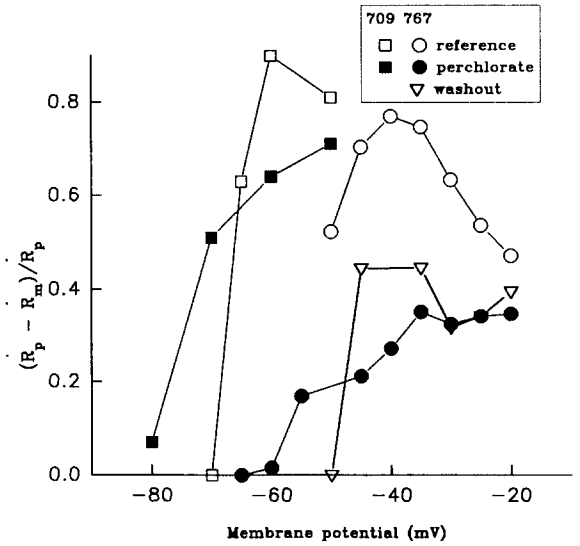

FIGURE 12. Perchlorate reduces fractional inactivation of release. Fractional inactivation of release flux, calculated as $(\dot{R}_p - \dot{R}_m)/\dot{R}_p$ for the saponin-treated fiber 767 (*circles* and *triangles;* computed from the records shown in Fig. 9) and fiber 709 (*squares;* release records in Figs. 11 and 16), permeabilized by notching.

records reveal kinetic effects due to ClO_4^-. The inset shows that the linear capacitance did not change significantly while in ClO_4^-, removing a possible source of error in studies of changes in threshold charge.

Fig. 14 shows the charges moved in ON and OFF as a function of voltage and, in the lower panel, the relationship between $\dot{R}_m$ and charge transferred. For several reasons we focused on $\dot{R}_m$ rather than $\dot{R}_p$. Most importantly, the steady value may be less affected by Ca^{2+}-dependent activation and inactivation processes and may be more simply associated with voltage and charge movement. Other reasons are operational—the value of the maximum is the result of rapid activation and inactivation processes—and hence susceptible to kinetic changes. Additionally, the steady value is always well defined, while the peak of release is many times nonexistent; moreover, it can be reduced or eliminated with conditioning pulses, a procedure used to advantage in the third article of this series. Finally, the peak of

release occurs before the end of the charge movement transient, which constitutes a problem as only the charge movement that precedes the peak could be causally linked with its level.

The plots in Fig. 14 *B* demonstrate reduction in Q_{th}. The charge moved in ClO_4^- at −65 mV was 2.4 nC/μF less than in reference at −50 mV (although the release elicited was greater), and the same can be said of the records at −60 mV in ClO_4^- and

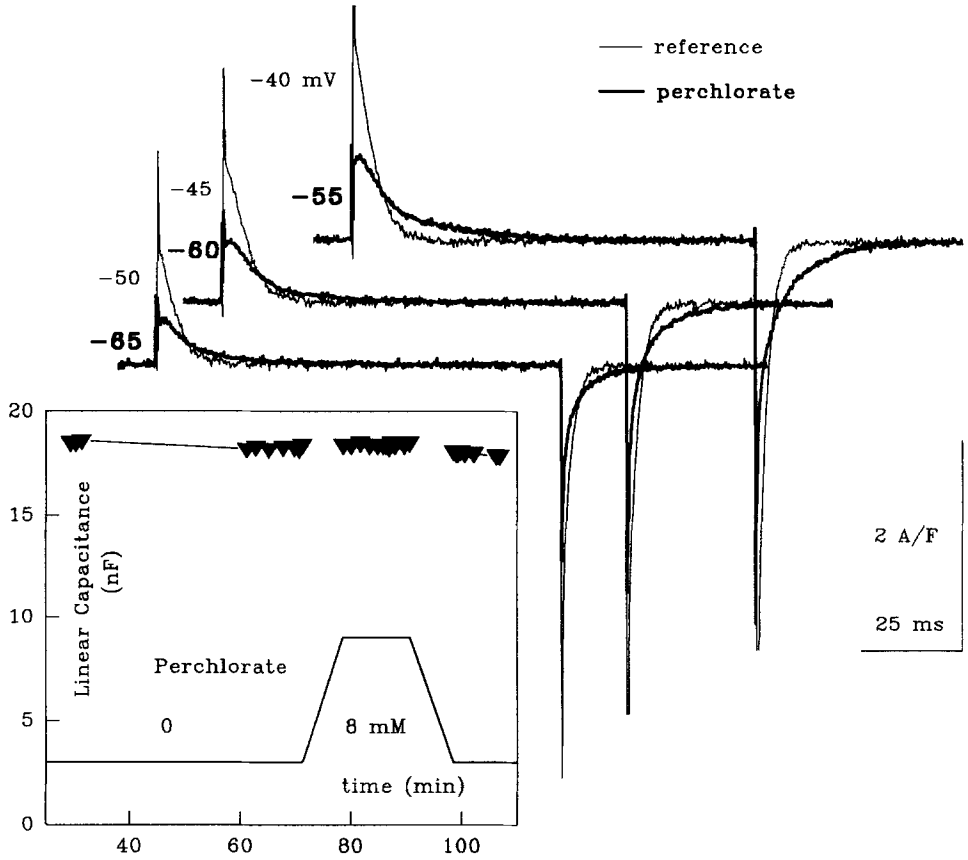

FIGURE 13. Charge movement currents in a saponized fiber. Same experiment as in Figs. 7–12. Records of asymmetric current were corrected by subtraction of a baseline fitted after the first 70 ms of the transients. Averages of two test and six control sweeps. (*Inset*) Time course of linear capacitance measured in the control currents.

−45 mV in reference. $\dot{R}_m(-55)$ in ClO_4^- is more than twofold greater than $\dot{R}_m(-40)$ in reference, but the charge moved is also greater, corresponding with the greater steepness due to ClO_4^-.

Measurements of threshold charge and its change by ClO_4^- were carried out in seven experiments with notched fibers. One of them (709) is illustrated in Figs. 15–17. The charge movement currents are in Fig. 15. This is an example of a fiber

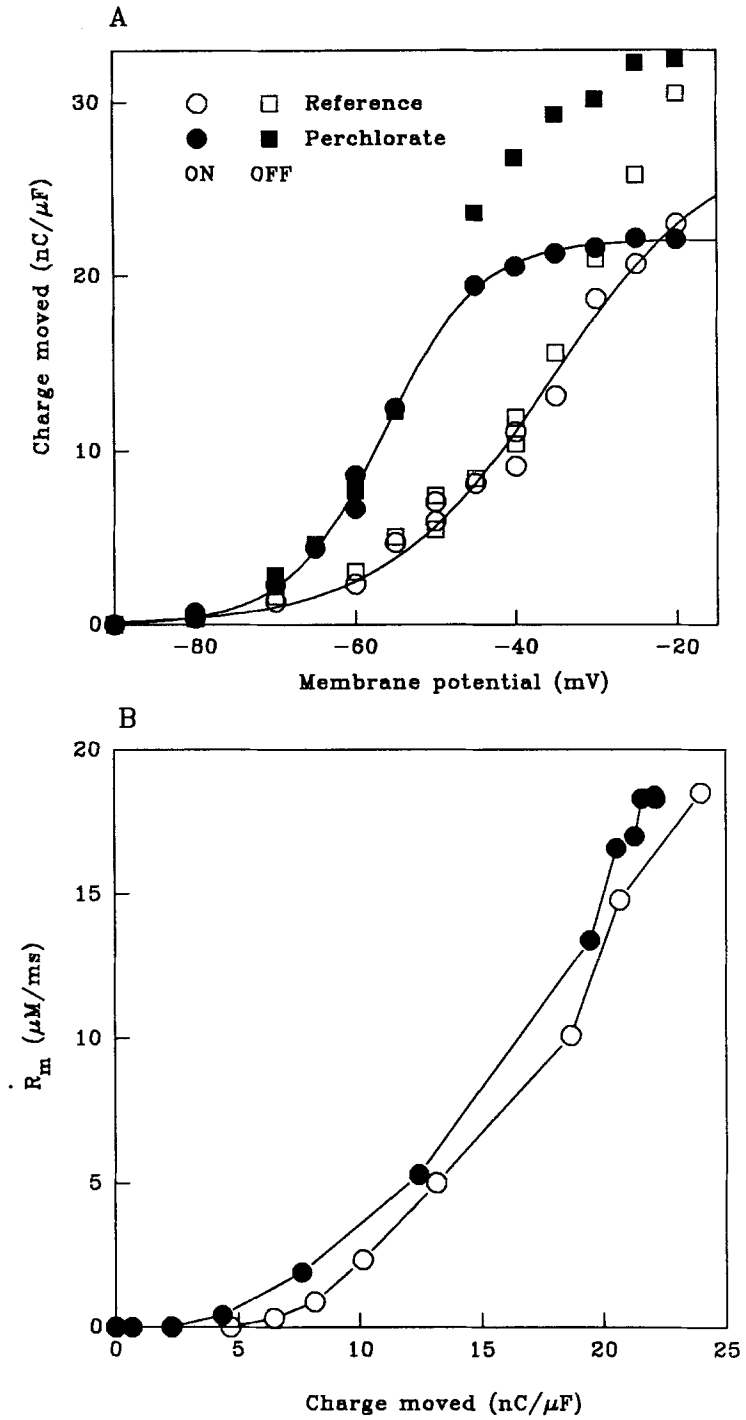

FIGURE 14. Dependence of Ca release flux on charge transferred. (*A*) Voltage dependence of charge moved, calculated from the records in the previous figure and other records not shown. *Continuous lines,* Boltzmann fits to ONs only. Parameters are listed in Table II. (*B*) Minimum of release flux ($\dot{R}_m$) vs. charge transferred. The values are the same as those represented by large circles in Figs. 10 *B* (release) and 14 *A* (charge).

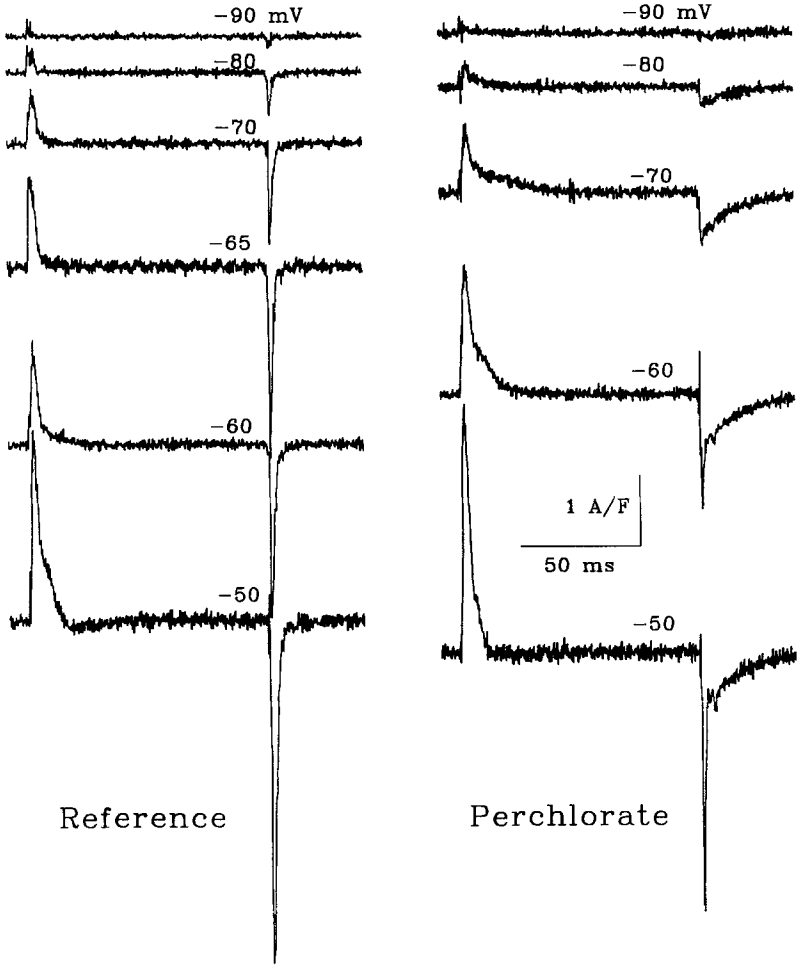

FIGURE 15. Charge movement currents in a notched fiber. Test currents were recorded during 100-ms pulses from a HP of −100 mV to the voltages indicated, and controls were taken between −120 and −100 mV. Shown are the asymmetric currents after subtracting a baseline fitted to the last 40 ms of the ON and OFF transients (100 ms of the OFF is not shown). Fiber 709. External solution, *Ca;* internal, *8 EGTA;* diameter, 70 μm; linear capacitance ranged between 19.1 and 20.7 nF in reference and between 20.7 and 21.6 nF in ClO_4^-. Temperature, 10°C.

with a small Q_γ hump in reference (at −60 and −50 mV), which is made greater and is made to appear at more negative voltages by ClO_4^-. An additional interesting observation, made repeatedly, is that ClO_4^- abolishes (reduces in other cases) a well-developed inward phase in the asymmetric current in reference (−50 mV). An increase in I_β and prominent kinetic effects at the OFF are often seen.

The $\dot{R}(t)$ records are represented in Fig. 16 and show similar characteristics and effects of ClO_4^- as in the saponin-treated fiber shown earlier. Fig. 17 summarizes quantitative aspects of this experiment. The $Q(V)$ is plotted in *A* and shows that the

voltage dependence of this experiment was shifted to more negative values even in reference. Even though the exploration was not taken beyond −50 mV (due to large Ca currents) the shift of $Q(V)$ caused by ClO_4^- is clear. $\dot{R}_m$ is plotted in Fig. 17 *B*, again showing a shift in the presence of ClO_4^-. As in Fig. 10 and in all other cases the shift in $\dot{R}_m(V)$ was greater than that of $\dot{R}_p(V)$ (not shown) and appeared to be greater than that of $Q(V)$. Fig. 17 *C* plots $\dot{R}_m$ and Fig. 17 *D* plots the corresponding value after correction for depletion versus ON charge moved during the same pulses. In this and all other experiments with notched fibers the dependence $\dot{R}_m(Q)$ was adequately described by a linear function that intercepts the charge axis at a positive value. The x intercept of the fitted line is used hereafter as the definition of threshold charge Q_{th}. In this experiment Q_{th} was 4.4 nC/μF in reference and 2 nC/μF in

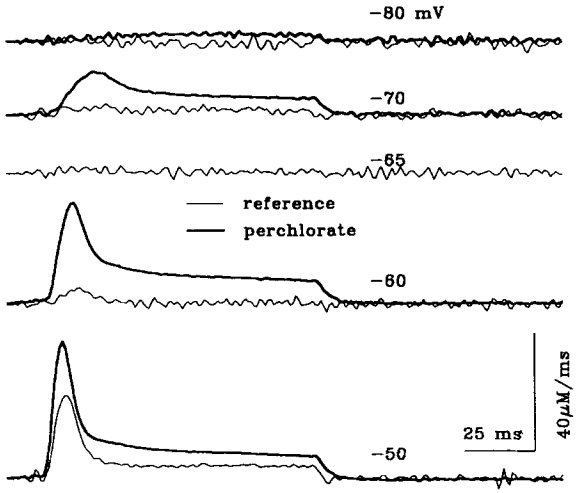

FIGURE 16. Calcium release flux in a notched fiber. Calcium release fluxes were calculated from the Ca^{2+} transients (recorded simultaneously with the currents shown in the previous figure) by the procedures described in Methods. The removal model was fitted to the records in ClO_4^- only, and the fit was applicable to the records in reference. Parameters of removal: $k_{OFF\,C_aT}$, 1,200 s^{-1}; $k_{ON\,C_aT}$, 130 $\mu M^{-1}\,s^{-1}$; $k_{OFF\,C_aP}$, 1.0 s^{-1}; $k_{ON\,C_aP}$, 100 $\mu M^{-1}\,s^{-1}$; $k_{OFF\,M_gP}$, 2.0 s^{-1}; $k_{ON\,M_gP}$, 0.03 $\mu M^{-1}\,s^{-1}$; M, 2.4 mM s^{-1}; $K_{D\text{-}pump}$, 0.5 μM; [pump], 100 μM; [P], 500 μM; [T], 120 μM; $[Mg^{2+}]$, 900 μM; [EGTA], 8 mM; $k_{ON\,C_a\,EGTA}$, 2.4 $\mu M^{-1}\,s^{-1}$; $k_{OFF\,C_a\,EGTA}$, 1.7 s^{-1}. The concentration of antipyrylazo III ranged between 362 μM at the beginning and 860 at the end of the series, which took 71 min. The records presented in Fig. 11 *B* are smoothed versions of the reference records at −65 and −60 mV and the record in ClO_4^- at −80 mV. The records shown were corrected for depletion as described in Eq. 1 and used to generate the data on fractional inactivation plotted as squares in Fig. 12.

ClO_4^-. In all cases we calculated Q_{th} before and after correction for Ca depletion in the SR, but the correction had little effect as the value of Q_{th} depends largely on the values of $\dot{R}_m$ at low voltages, and these are not affected by the correction.

ClO_4^- reduced by ~2.5 nC/μF the charge Q_{th} in both experiments illustrated. The point was explored in the same way in six other experiments. The results are listed in Table IV. On average, Q_{th} was reduced from 6.0 nC/μF (SEM 0.4) to 3.4 nC/μF (SEM 0.5). The average of paired differences was 2.8 nC/μF (SEM 0.3), a highly significant reduction ($P < 0.001$). Charge in the controls was not significantly changed. Later in this article and in the third article of this series we present additional experiments, under different conditions, which also show reductions in Q_{th} in the presence of ClO_4^-.

Ca Depletion Simplified the Effects of Perchlorate

As we have seen, ClO_4^- causes an increase in Q_γ, judging from either the kinetic changes or the increase in steepness of the $Q(V)$ dependence. Csernoch et al. (1991) have shown that interfering with Ca release reduces or suppresses the Q_γ component.

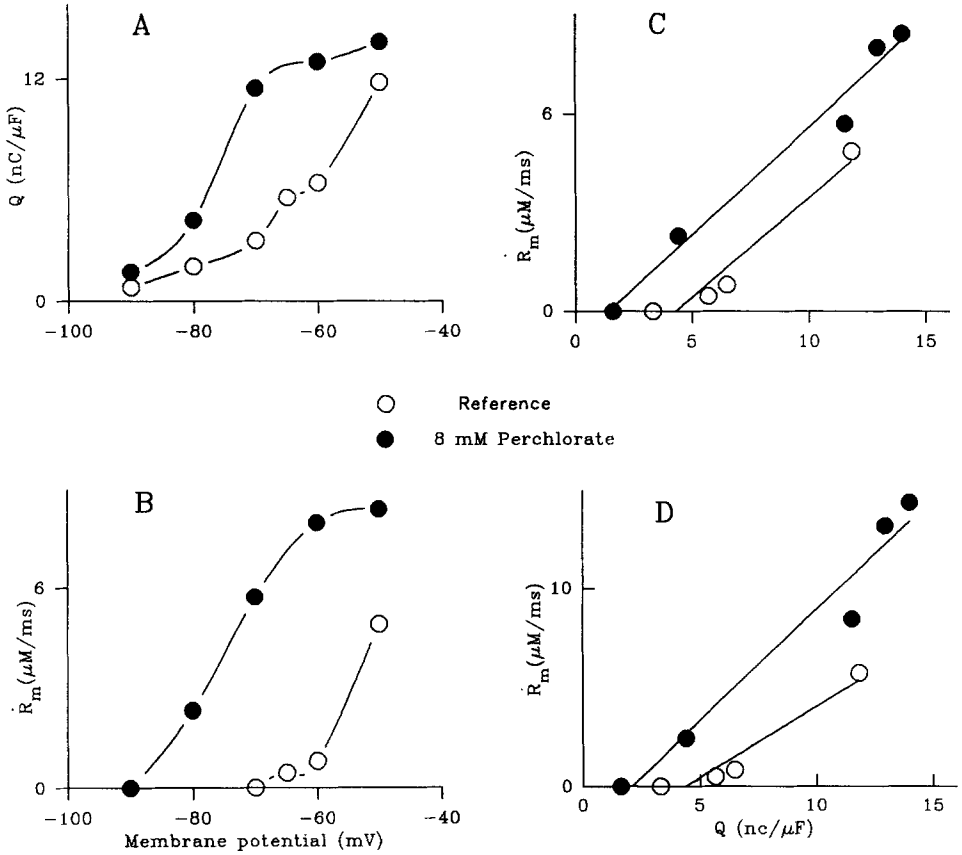

FIGURE 17. Voltage and charge dependence of release flux. (*A*) Voltage dependence of charge moved in reference (*open circles* in all graphs of this figure) and in 8 mM ClO_4^- (*filled circles*). The line is a cubic spline. (*B*) Voltage dependence of the minimum value of release flux (which is equal to the steady value at the end of the pulse in all cases except the reference at −60 mV). (*C*) Minimum release flux (ordinate values of *B*) as a function of charge moved (from *A*). Lines are linear fits to each set of points. (*D*) Minimum release flux corrected for depletion. Fiber 709. Other details are given in Figs. 15 and 16.

García, Pizarro, Ríos, and Stefani (1991) demonstrated that depletion of Ca in the SR reduced or eliminated the hump. Those results, and the Ca-binding model proposed to explain them (Pizarro et al., 1991*b*), suggest that some of the effects of ClO_4^-, and in particular the increase in Q_γ, may be secondary to an increase in Ca release.

A better understanding of the primary effect requires the elimination of possible

secondary effects. Consequently, we set out to study the ClO_4^- effects on depleted fibers. Initially we applied the procedure of pulsing the fibers equilibrated with an internal solution with *30 EGTA* and no added Ca (García et al., 1991). In these experiments we could only obtain partial and rapidly reversible depletion, not what we needed for a study of ClO_4^- effects on both kinetics and voltage dependence of charge and release flux.

We therefore tried other approaches to achieve more radical buffering. We added 1 or 3 mM BAPTA to *15 EGTA* internal solution. BAPTA, which appears to have a much faster Ca binding rate than EGTA, should reduce more effectively the rise in $[Ca^{2+}]_i$ at early times, thus minimizing the reuptake into the SR and hastening depletion. There is another reason to use BAPTA. The rationale for causing depletion is to reduce the hypothetical feedback of released Ca on the voltage

TABLE IV

Effect of 8 mM Perchlorate on Threshold Charge Movement

Fiber No.	Qth		
	Reference	Perchlorate	Differences
		nC/μF	
689	6.2	1.8	4.4
692	5.1	3.0	2.1
709	4.4	2.0	2.4
712	5.5	3.6	1.9
727	7.3	5.1	2.2
728	7.3	4.8	2.5
738	7.0	4.3	2.7
767	4.8	2.4	2.4
Average	6.0	3.4	2.8
SEM	0.4	0.5	0.3

All experiments except 709 and 767 were conducted in external *Ca* and internal *15 EGTA* (709 was in *8 EGTA* and 767 was in *30 EGTA*). Threshold charge Q_{th} was determined as the x intercept of a line fitted to $\dot{R}_m$ vs. Q plots. $\dot{R}_m$ was calculated on records corrected for depletion following eq. 1. When there were several points (obtained at different subthreshold test voltages) of $\dot{R}_m = 0$, only the ones at the highest voltage were used in the fit. For 767 only the first three nonzero points were used in the determination of Q_{th}.

sensors. The presence of BAPTA should reduce directly the feedback mediated by free Ca^{2+}, even if it failed to cause complete depletion.

The results of the experiments are illustrated in Figs. 18–21. The Ca transients recorded in a fiber after exposure for 23 min to a *15 EGTA* internal solution with 1 mM BAPTA are in Fig. 18 *A*. In spite of the high buffering there were measurable Ca transients. The voltage dependence of release seems to be shifted to higher voltages, an observation made in all fibers exposed to intracellular solutions with BAPTA.

The fiber was then subjected to a series of 200 pulses of 50 ms to +20 mV, one pulse every 12 s, a pattern expected to cause substantial depletion. Test pulses applied after this treatment generated the Ca transients of Fig. 18 *B*. The calculated release fluxes are plotted in Fig. 19 *C* and the asymmetric currents in Fig. 20.

The OFF portions of the Ca^{2+} transients in ClO_4^- in Fig. 18 *A* (plus others not shown) were fitted extremely well if the removal model included, in addition to 15 mM EGTA, a rapidly equilibrating compartment representing a binding site of dissociation constant 100 nM, at a concentration of 1 mM (representing BAPTA). All parameter values are listed in the legend to Fig. 19. Fig. 19 shows the release records

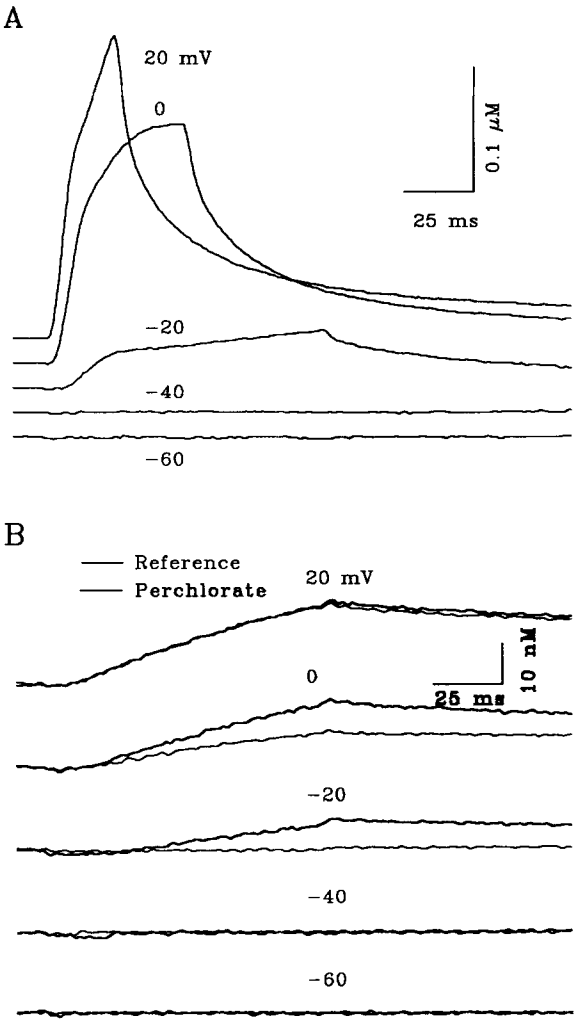

FIGURE 18. Calcium transients and depletion. (*A*) Calcium transients elicited by pulses to the voltages indicated from a HP of −80 mV. External solution, Ca; changed to *Ca-Co* after depletion; internal, *15 EGTA* plus 1 mM BAPTA and no added calcium. The fiber had been exposed to this internal solution for 33 min and pulsing was sparse, separated by 1–2-min intervals. Antipyrylazo III went from 340 to 500 μM during the sequence, which took 12 min. (*B*) Calcium transients elicited by pulses to the same potentials after subjecting the fiber to a prolonged depleting pulse protocol (200 pulses to +20 mV at 12-s intervals; the timing of pulses and depletion protocols is illustrated in Fig. 19). The records in reference (*thin traces*) were obtained before the records in ClO_4^- (8 mM). The sequence took 10 min in reference and 17 min in 8 mM ClO_4^-. The concentration of antipyrylazo III ranged from 768 μM when applying the depletion protocol, to 1.4 mM before changing to ClO_4^-, and to 2.40 mM after 15 min of washout at the end of the series. Fiber 774. Diameter, 118 μm. Temperature, 10°C.

before (*A*) and after depletion (*C*). Fig. 19 *B* illustrates the timing of application of the depletion protocol, its effect on Ca_{SR}, and its lack of effect on the linear capacitance. It is interesting to note that the release records were of normal features initially, even though high BAPTA was present inside the fiber (as revealed by the remarkable change in shape of the Ca^{2+} transients (cf. Methods). After depletion,

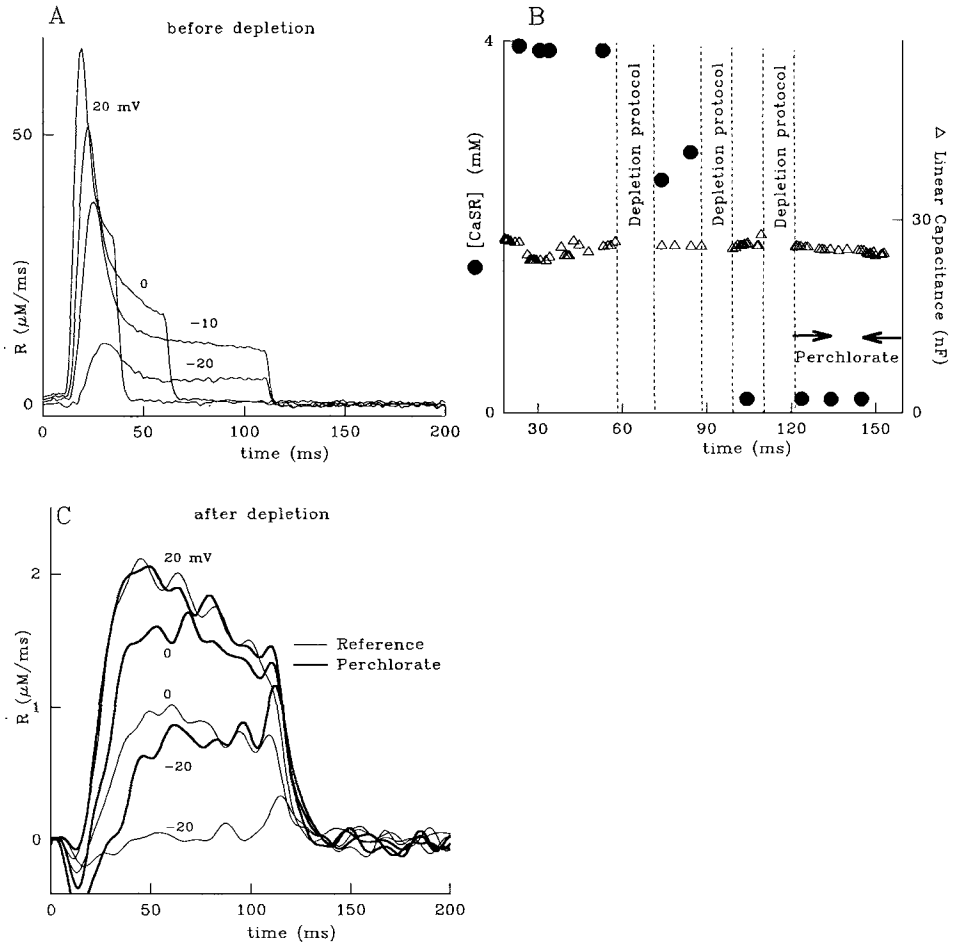

FIGURE 19. Release flux and depletion. (*A* and *C*) Release flux records calculated from the Ca^{2+} transients in Fig. 18. To fit the Ca^{2+} transients, a Ca^{2+} binding compartment in rapid equilibrium, at a concentration of 1 mM and with a K_D of 100 nM, was added to the removal model. Note the similarity between the records in *A* and those of Figs. 3, 9, and 16, in spite of the very different Ca^{2+} transients. (*B*) Time course of Ca_{SR} (*circles*) and linear capacitance (*triangles*). Ca_{SR} was calculated using the depletion correction procedure described before (except the lowest values, 0.15 mM, which were estimated from the ratio of releases before and after depletion). The vertical lines mark the times of application of the depletion protocol (50-ms pulses to +20 mV; 40, 100, and 60 pulses, respectively, in the three intervals). The horizontal arrows mark the interval in ClO_4^- (8 mM). Parameters of removal: $k_{OFF\,C_a\,P}$, 1.0 s^{-1}; $k_{ON\,C_a\,P}$, 100 μM^{-1} s^{-1}; $k_{OFF\,M_g\,P}$, 7.0 s^{-1}; $k_{ON\,M_g\,P,\ 0.03\ \mu M^{-1}}$ s^{-1}; M, 3.0 mM s^{-1}; K_{Dpump}, 0.3 μM; [pump], 100 μM; [P], 250 μM; [Mg^{2+}], 900 μM; [EGTA], 15 mM; $k_{ON\,C_a\,EGTA}$, 6.2 μM^{-1} s^{-1}; $k_{OFF\,C_a\,EGTA}$, 2.3 s^{-1}. [BAPTA], 1 mM; $k_{ON\,C_a\,BAPTA}$, 1,000 μM^{-1} s^{-1}; $k_{OFF\,C_a}$ BAPTA, 100 s^{-1} (giving a K_D of 100 nM and fast equilibration). Troponin, from 0 to 200 μM, with its usual kinetic parameters, did not significantly change the goodness of the fit or the computed release fluxes. The same parameters gave a good fit before and after depletion.

however, the Ca transients became ramp-like, almost linear increases; correspondingly, the release records essentially lost their inactivating component.

Fig. 20 first shows the effect of the depletion protocol on the charge movement currents (inset). The modest hump present was essentially eliminated, as was a small

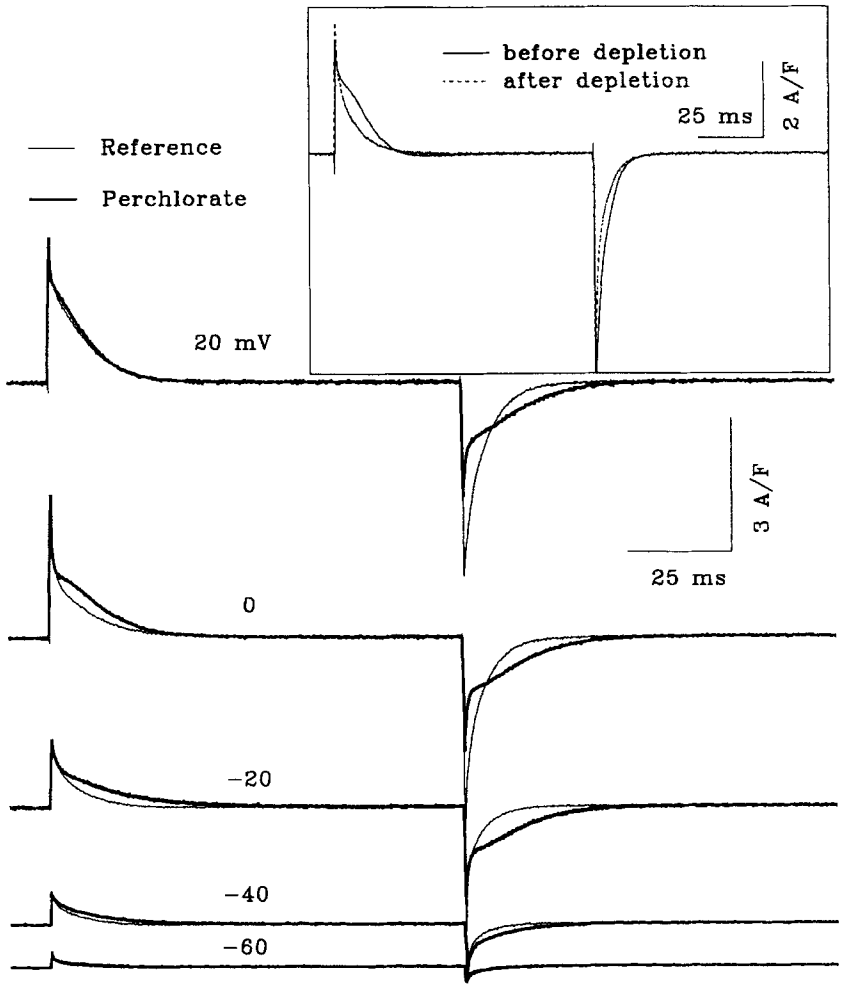

FIGURE 20. ClO_4^- has kinetic effects on charge movement regardless of depletion. *Thin traces,* charge movement records obtained after depletion, simultaneously with the calcium transients in Fig. 18 *B*. *Thick traces,* corresponding records in 8 mM ClO_4^-. (*Inset*) Records at −10 mV, before (*continuous line*) and after the depletion protocol (*dashed line*). Asymmetric currents were corrected by baseline subtraction. Averages of two tests and four control sweeps. Linear capacitance is plotted in Fig. 19 *C*.

inward phase that followed the hump at some voltages (inset). Neither the Ca transients nor the charge movement reverted to their early form for ~10 min after the depleting pulse series. During that time the reference records shown in Figs. 18 *B* and 20 were obtained.

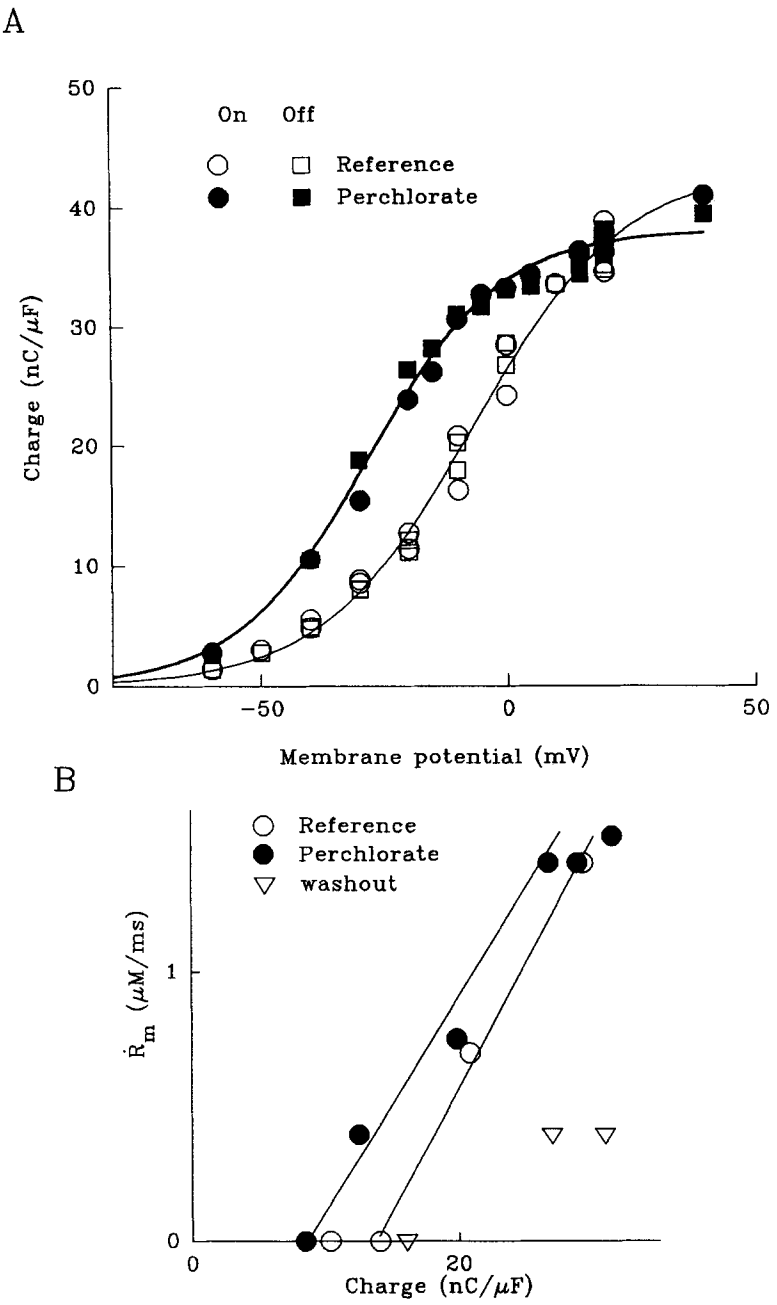

FIGURE 21. Effect of ClO_4^- on $Q(V)$ and $\dot{R}(Q)$ of depleted fibers. (*A*) Charge moved after applying the depletion pulse protocol as a function of test pulse voltage. Lines are single Boltzmann terms fitted to ON and OFF points. Same experiment of the previous figures. Best fit parameters are listed in Table V. (*B*) $\dot{R}_m$ vs. charge transfer. $\dot{R}_m$ values in reference and ClO_4^- were calculated from Fig. 19 *B* and washout values (*triangles*) from records not shown. Linear functions were fitted to the points. The two high voltage points in ClO_4^- were obtained at the end of the lapse and were not considered in the fit.

After obtaining the reference records the external solution was replaced with one containing 8 mM ClO_4^- and the pulses were repeated. Ca^{2+} transients are represented in Fig. 18 *B*, release records in Fig. 19 *C*, and charge movement records in Fig. 20 (thick traces). ClO_4^- still induced major changes. The Ca transients were changed: the threshold shifted by some 20 mV and the amplitude increased except at the highest voltage. The kinetics of the transients remained unchanged. ON charge movements were increased at all voltages except the highest (consistent with the changes in Ca^{2+} transients). The kinetics of charge movement were slowed and became nonexponential both in ON and OFF.

Fig. 21 *A* plots the total charge transferred after depletion in both ON and OFF (circles and squares, respectively) in reference (open symbols) and ClO_4^- (filled symbols). The curves represent single Boltzmanns, fitted to both ON and OFF values

TABLE V

Effect of Perchlorate on the Q(V) Distribution of Depleted Fibers

Fiber No.	Perchlorate	Q_{max}	Differences	K	Differences	V	Differences
	mM	*nC/μF*		*mV*		*mV*	
774	0	43		15.4		−7	
	8	37	−6	12.5	−2.9	−28	−21
778	0	38		15.2		−12	
	8	36	−2	13.9	−1.3	−32	−20
784	0	29		13.0		−21	
	8	28	−1	16.7	3.7	−29	−8
883	0	43		12.5		−26	
	8	43	0	10.7	−1.8	−38	−12
884	0	37		10.6		−29	
	8	40	3	9.8	−0.8	−41	−12
Average			−1.2		−1.7		−14.7
SEM			1.5		0.45		2.6

Experiments 774, 778, and 784 were conducted in external *Ca-Co* and internal *15 EGTA* plus 1 mM BAPTA (774) or 3 mM BAPTA (778 and 784). 883 and 884 were in external solution *Co* and internal *60 EGTA*. In all cases, before the measurements the fibers were pulsed ~200 times to +20 mV at 10–12-s intervals. Averages of fit parameters, respectively, in reference and ClO_4^-: Q_{max} (nC/μF), 38 (2.6), 37 (2.5); K (mV), 13.3 (0.9), 12.7 (1.2); $\overline{V}$ (mV), −19 (4.2), −34 (2.5).

of charge moved. After the depleting intervention, ClO_4^- still caused a large negative shift in $\overline{V}$, but only a small increase in steepness. As before, Q_{max} remained the same. Two other experiments had almost identical results, including the observation of ramp-like Ca transients (noninactivating fluxes of Ca release).

The effects of ClO_4^- on the voltage distribution of intramembrane charge in three experiments in fibers depleted in the simultaneous presence of EGTA and BAPTA are listed in Table V. Additionally, we carried out two experiments without BAPTA to rule out the possibility of a specific pharmacological effect. We could deplete Ca in the SR using an internal solution with 60 mM EGTA, no added calcium, and an external solution with no Ca^{2+} (*Co*, Table I), using a similar train of pulses to cause depletion. The experiments carried out in this manner had results similar to the ones

with BAPTA and are included in Table V. ClO_4^- caused an average shift in $\overline{V}$ of −15 mV, a slight reduction in K (by 1.7 mV), and no change in Q_{max}.

In the experiments with intracellular BAPTA we also explored the relationship between Ca release and charge movement. Since there was very little inactivating component of Ca release, $\dot{R}_m$ was well defined; it is plotted vs. charge transferred in Fig. 21 *B*. As in the experiments in nondepleted conditions described earlier, there was a substantial shift of the relationship to lower values of charge after ClO_4^-, and a consequent reduction in Q_{th} (by 6.3 nC/μF).

Unlike previous experiments in nondepleted fibers, the relationship in ClO_4^- curved downward at high voltages. The charge transfer and linear capacitance remained at similar values, indicating that the reduction in $\dot{R}_m$ was not due to terminal deterioration. This could be a consequence of the increase in depletion in ClO_4^-. Alternatively, it could be a consequence of the entry of cobalt after a prolonged experiment. Consistent with either possibility, the release flux calculated after washout (triangles) was threefold smaller than in reference. The conclusion that Q_{th} was reduced by ClO_4^- relies on measurements at lower voltages, which were made earlier and are therefore less susceptible to the late decrease in signal. Furthermore, the errors considered above would have made Q_{th} appear greater, not smaller, in ClO_4^-. Thus, the conclusion that Q_{th} is reduced by ClO_4^- is not affected by this reduction in the signal.

The Effects of Perchlorate Are Reversible after a Lag

The effects of ClO_4^- were reversible, as illustrated, for example, by the recovery of the voltage dependence of $\dot{R}_p$* after washout in the experiment of Fig. 10. The kinetics of onset and recovery were explored in three experiments in which the levels of ClO_4^- were changed several times, while its effects were monitored with the same pulse applied frequently at regular intervals. One such experiment is illustrated in Fig. 22. After an interval in reference the fiber was exposed to 1 mM ClO_4^- and the lower concentration was chosen to facilitate washout. After 7 min in this solution, ClO_4^- was washed out by flushing with a volume of reference solution 15-fold greater than that of the external pool. After an interval in this solution the procedure was repeated with 2 mM ClO_4^-. A 100-ms pulse to −30 mV and corresponding controls were applied repeatedly. The linear capacitance remained stable throughout and there was little evidence of SR depletion during the pulses (although release flux at the end of the series was about half of that at the beginning).

The graph shows that both levels of ClO_4^- increased the charge transferred (circles), the minimum release level (which was attained at the end of the pulse [squares]), and the OFF time constant of charge movement (triangles). The changes were reversible. Their onset started immediately after exposure to ClO_4^- but seemed to take a few minutes to reach completion in both concentrations of ClO_4^-. More strikingly, their recovery after washout was very slow and exhibited a lag. This is especially clear after the interval in 2 mM ClO_4^-, as the first two values of charge transfer, release and τ, obtained 1 and 3 min after washout, were virtually identical (something similar occurred after 1 mM ClO_4^- but the changes in τ were less clear). Even though the time taken to change solutions limits our ability to evaluate the time

course of the effects, in all three experiments the effects appeared immediately and the recovery seemed slower and started after a lag.

Effects of Perchlorate on Charge 2

In previous sections we showed that some of the effects of ClO_4^- require the existence of substantial Ca release and some do not. In this section we explore the possible requirement of a functional interaction between voltage sensor and release channel for the effects of ClO_4^-. With this intention we looked for effects of the anion on charge 2, under the assumption (Brum and Ríos, 1987; Caputo and Bolaños, 1989; reviewed by Ríos and Pizarro, 1991) that charge 2 results from conformational

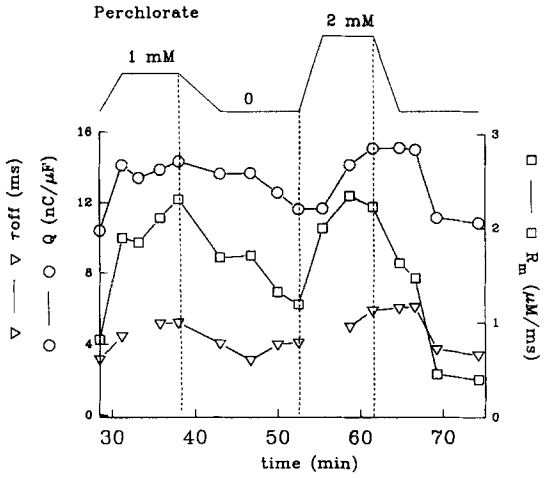

FIGURE 22. Onset and reversal of the effects of ClO_4^-. Effects of ClO_4^- were monitored with 100-ms pulses to −20 mV (two tests and four controls per average, from a HP of −80 mV). No pulses were applied other than those indicated in the plots. The left side ordinate applies to both charge transferred (*circles*) and its OFF time constant (*triangles*). The two missing τ values correspond to noisy charge movement records that did not give a good single exponential fit. The plot of perchlorate level (*top*) represents by sloping lines the times of solution change. Parameters of removal: $k_{OFF\,C_aT}$, 1,200 s^{-1}; $k_{ON\,C_aT}$, 130 $\mu M^{-1}\ s^{-1}$; $k_{OFF\,C_aP}$, 1.0 s^{-1}; $k_{ON\,C_aP}$, 100 $\mu M^{-1}\ s^{-1}$; $k_{OFF\,M_gP}$, 13 s^{-1}; $k_{ON\,M_gP}$, 0.03 $\mu M^{-1}\ s^{-1}$; M, 2.5 mM s^{-1}; K_{Dpump}, 1.0 μM; [pump], 100 μM; [P], 1 mM; [T], 240 μM; [Mg^{2+}], 900 μM; [EGTA], 8 mM; $k_{ON\,C_aEGTA}$, 2.0 $\mu M^{-1}\ s^{-1}$; $k_{OFF\,C_aEGTA}$, 5.0 s^{-1}. The concentration of antipyrylazo III ranged between 354 μM at the beginning and 875 μM at the end of the series. Fiber 826. External solution, *Ca;* internal solution, *15 EGTA*. Diameter, 93 μm. Linear capacitance fluctuated between 31.8 and 30.7 nF, not correlated with the ClO_4^- levels. Temperature, 12°C.

transitions among inactivated states of the voltage sensor. Since the inactivated voltage sensors fail to cause Ca release, any effect of ClO_4^- on charge 2 would not require the functional interaction of EC coupling.

Asymmetric currents recorded in a fiber held (inactivated) at 0 mV are shown in Fig. 23 *A* and the currents after baseline subtraction are shown in Fig. 23 *B*. The effect of 8 mM ClO_4^- (thick traces) includes suppression of a small early phase during the ON, and not much else. ClO_4^- is a known blocker of muscle Cl channels (Bretag, 1987); the inward asymmetric current in depolarized fibers contains a component that is blockable by 1 mM anthracene 9-carboxylate (Csernoch et al., 1991; Szücs,

Papp, Csernoch, and Kovács, 1991). Therefore, the inward current blocked by ClO_4^- is likely to flow through Cl channels.

The charge transferred is plotted in Fig. 24. Note that the ON and OFF values in reference were similar at all but the most negative voltages (which may be a fortuitous

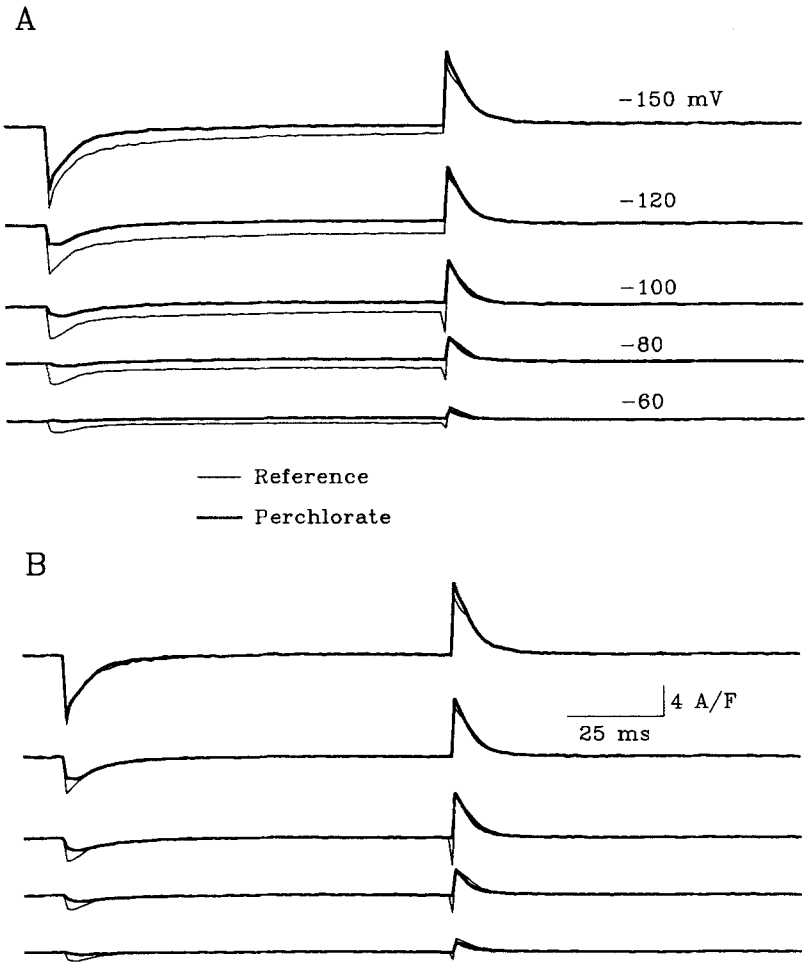

FIGURE 23. Effects of ClO_4^- on charge 2 currents. (*A*) Asymmetric currents and (*B*) currents after baseline subtraction. Test pulses went to the voltages indicated from a HP of 0 mV. Control pulses went from HP to 40 mV. The first point (1 ms) of all ON records and the OFFs at −120 and −150 mV was large and inverted and is not shown. Fiber 787. External solution, *Co;* internal solution, *15 EGTA* with 3 mM BAPTA and no added calcium. Diameter, 86 μm. Linear capacitance, 11.5 nF. Temperature, 10°C.

cancellation of a small ionic current present in the ON and a failure of the correction and integration to include all of the ON charge). In view of the ionic component present at the ON, the Boltzmann functions were fitted to OFF values only. ClO_4^- shifted $\overline{V}$ by −16 mV without causing other changes in the Boltzmann parameters.

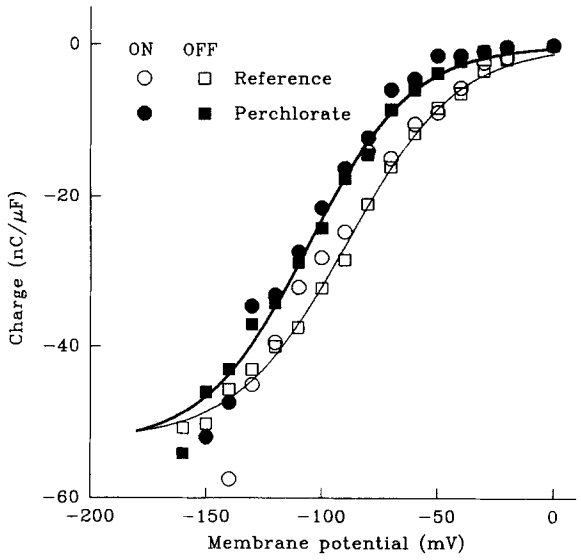

FIGURE 24. Effects of ClO_4^- on the voltage distribution of charge 2. Time integrals of the records in Fig. 23 *B*. Lines generated with single Boltzmann terms fitted to all OFF values, with the exception of the OFF value in ClO_4^- at −160 mV. Best fit parameters listed in Table V.

This was the case in six experiments, listed in Table VI. Of those, the first four were carried out in 1988 (with Dr. G. Pizarro and Dr. I. Uribe) with the standard solutions used by Brum and Ríos (1987) in their study of charge 2. Experiments 787 and 788 were carried out in external *Co* and internal *15 EGTA* solutions, and their transition

TABLE VI

Effect of Perchlorate on Charge 2

Fiber No.	Perchlorate	Q_{max}	Differences	K	Differences	$\overline{V}$	Differences
	mM	*nC/μF*	*nC/μF*	*mV*	*mV*	*mV*	*mV*
348	0	44		23		−123	
	7	47	3	29	6	−130	−7
349	0	52		21		−120	
	7	50	−2	18	−3	−125	−5
350	0	45		18		−103	
	7	51	6	18	0	−120	−17
351	0	40		21		−107	
	7	43	3	22	1	−129	−22
787	0	52		23		−89	
	8	53	1	22	−1	−105	−16
788	0	60		25		−96	
	8	61	1	23	−2	−112	−16
Average			2.00		0.17		14*
SEM			1.10		1.30		2.65

Boltzmann fits to $Q(V)$ data in fibers held depolarized at 0 mV. Only OFF values were used. Fibers 348, 349, 350, and 351, and external and internal solutions were the standard solutions used by Brum and Ríos (1987) in the study of charge 2. External solution is similar to *Ca* (Table I) but with 2 mM [Ca^{2+}] (TEA substituted for Ca). Internal solution is similar to the internal solutions in Table I but with 0.1 mM EGTA (glutamate substituted for EGTA) and a nominal [Ca^{2+}] of 50 nM. Fibers 787 and 788: external *Co*, internal *15 EGTA* plus 3 mM BAPTA and no added Ca.

voltage was substantially higher than that of the earlier experiments. In all of them ClO_4^- caused a negative voltage shift and no other major changes. On average $\overline{V}$ was shifted by −14 mV ($P < 0.01$).

Charge 2 did not slow its kinetics under ClO_4^- in any of the experiments listed in Table VI. This was also true in six other experiments of the same earlier series in which a higher concentration of ClO_4^- (20 mM) was used.

Cl Channel Blockers Do Not Change the Kinetics of Charge Movement

The latter experiments, which revealed a Cl channel blocking effect of ClO_4^-, raised the possibility that the voltage shift induced by ClO_4^- was linked to its channel

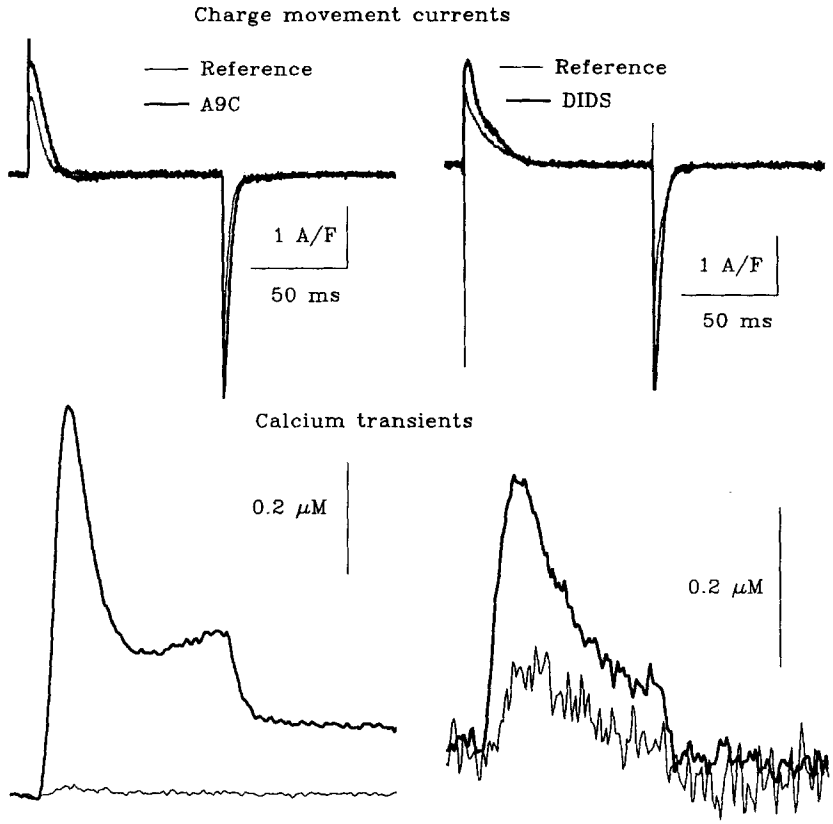

FIGURE 25. Effects of a Cl channel blocker. Records of asymmetric current (*top*) and Ca transients, elicited by a slightly suprathreshold pulse in reference (*thin trace*) and in the presence of a Cl channel blocker (*thick traces*). (*Left*) The blocker is A9C (8 mM). Pulse to −45 mV (from a HP of −90 mV). Records are averages of two tests and four controls. Fiber 824. External solution, *Ca;* internal solution, *15 EGTA*. Dye concentration: 881 μM (reference) and 899 μM (A9C). Diameter, 108 μm. Linear capacitance, 21 nF. Temperature, 10°C. (*Right*) The blocker is DIDS (2 mM). Pulses to −50 mV (from −90 mV). Records are single sweeps with three controls. Fiber 834. Solutions were *Ca* and *8 EGTA*. Dye concentration: 288 μM (reference) and 434 μM (DIDS). Diameter, 96 μm. Linear capacitance, 18 nF. Temperature, 12°C.

blocking effect. Indeed, binding of extracellular anions to Cl channels or their partition in the bilayer should cause local depolarization and a shift to more negative voltages of any functions of nearby voltage sensors. For this reason we explored the effect of other Cl channel blockers, including A9C, SITS, and DIDS. Fig. 25 shows the effects of 8 mM A9C applied externally (left panels) and of 2 mM DIDS (right panels) on the asymmetric currents (top) and the Ca^{2+} transients (bottom) elicited in both cases by pulses that were just suprathreshold in reference. From the increment in the Ca^{2+} transients in the presence of the drugs and from records not shown, the voltage that caused minimum detectable release was shifted by about −10 mV by A9C and about −5 mV by DIDS. The charge movement currents are shown in the top panels, and in both cases the drugs caused an increase in charge transferred, roughly consistent with the change in threshold voltage revealed by the $[Ca^{2+}]$ measurements. The top records also show that the kinetics of charge movement were not changed significantly. The voltage for minimum detectable release was shifted between −4 and −15 mV in three experiments with 2 mM SITS, three experiments with 2 mM DIDS, and six experiments with A9C at concentrations ranging from 1 to 8 mM. Only minor changes in kinetics of charge movement were observed.

In summary, the Cl channel blockers decreased threshold voltage and increased charge movement at low voltages. These changes, consistent with a negative shift of $Q(V)$, were not accompanied by the kinetic changes induced by ClO_4^-.

DISCUSSION

This series of experiments has consequences that touch on a number of questions in EC coupling, and suggests probable sites of action of ClO_4^-. The Discussion will be divided into four sections. In the first we organize the various effects according to their requirements. In the second we discuss possible mechanisms of action, including a "chaotropic" theory of the effects. In the third, possible target sites for perchlorate are considered. Finally, we discuss the effects on Q_γ and their consequences.

The Various Effects of Perchlorate Have Different Requirements

The results demonstrate multiple effects of ClO_4^- on charge movement and Ca release, many of which have been described in previous work of other laboratories. New in this article is the study of the effects in different situations of the EC coupling system. The effects on normal EC coupling included: (*i*) a slowing of the OFF charge movement current, (*ii*) a change in $\bar{V}$ to more negative values, (*iii*) an increase in the steepness of $Q(V)$, (*iv*) a reduction in Q_{th}, (*v*) an increase in the hump of charge movement, (*vi*) a shift to more negative voltages of $\dot{R}_p(V)$ and $\dot{R}_s(V)$, (*vii*) a decrease and change in the voltage dependence of the fractional inactivation F_i, and (*viii*) a slow decrease in the Ca content of the SR. Of these, the first four are the main effects, and they will be referred to as $\Delta\tau_{off}$, $\Delta\bar{V}$, ΔK, and ΔQ_{th}. Effect *v* will be discussed later as a consequence of ΔQ_{th}; *vi* is another expression of the phenomenon that reduces Q_{th}; the discussion of effect *vii*, on the kinetics of Ca release, will be postponed until the following articles; and finally, the depletion effect, *viii*, may be another manifestation of increased readiness of Ca release to activate.

This set of effects was substantially simplified when the system was put in peculiar functional states. The consideration of these changes is best done in reference to the following diagram, where the three boxes represent three functional situations:

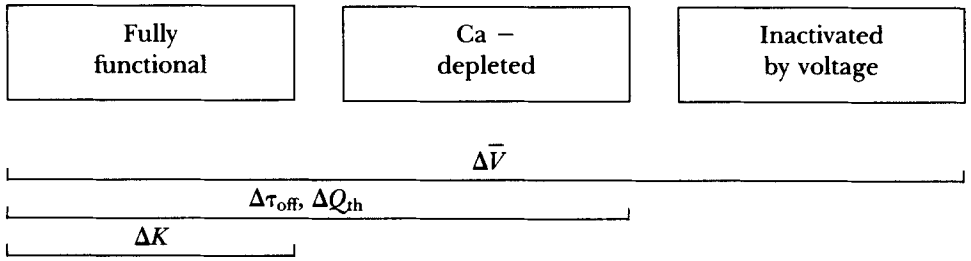

The brackets indicate the requirements of the various effects. $\Delta\bar{V}$ occurs in all conditions studied; ΔQ_{th} and $\Delta\tau_{off}$ were present only in noninactivated fibers, depleted or not; and ΔK, representing the approximately twofold change in steepness of $Q(V)$ and the increase in the hump or Q_γ, required Ca release and presumably the consequent increase in $[Ca^{2+}]_i$. In depleted fibers the increase in steepness was barely noticeable.

From the absence of requirements for the effect $\Delta\bar{V}$, and the observation of shifts in threshold voltage (by -4 to -15 mV) without other effects when the fibers were exposed to Cl channel blockers, we infer that at least part of the voltage shift is not related to the other effects and is probably a simple electrostatic consequence of anions partitioning in the membrane or binding near voltage sensors. A similar effect of Cl channel blockers on $Q(V)$ was described by Heiny, Jong, Bryant, Conte-Camerino, and Tortorella (1990).

The depletion protocol in BAPTA caused the disappearance of both visible humps in charge movement and of effects of ClO_4^- that can be loosely described as increase in Q_γ (the increase in hump and the twofold increase in steepness of $Q(V)$). This indicates that this effect, ΔK in the diagram, requires Ca^{2+} release. This implies that ΔK is not a direct or primary effect of ClO_4^-. It will be considered in detail below.

The two other effects in the diagram, ΔQ_{th} and $\Delta\tau_{off}$, are particularly interesting: they are both specific of ClO_4^- (not shared with the anionic channel blockers) and direct (not mediated by Ca release). The kinetic effect $\Delta\tau_{off}$ does not occur with charge 2; thus, the only effect of ClO_4^- on the inactivated voltage sensor is a voltage shift, which is probably due to binding to Cl channels. This agrees with a finding of Huang (1987), that the effect on τ_{off} was lost upon partial inactivation. The specificity of the direct effects of ClO_4^- for noninactivated states of the voltage sensor suggests either that the anion binds to the sensor with state-dependent affinity (a "modulated receptor" scheme) or that it binds on the release channel and alters the sensor via an allosteric interaction between sensor and channel.

Perhaps the most significant result here is what we term the ΔQ_{th} effect. It contradicts the study of Csernoch et al. (1987), who concluded that Q_{th} was not changed by ClO_4^-. In their case, Q_{th} was defined as the charge moved at the voltage that caused the minimum detectable movement, judged visually under the microscope. Our definition is arguably superior as it is based on measurements of Ca^{2+} transients rather than movement, and on extrapolations of linear dependencies fitted

over a range of voltages rather than single determinations of threshold. Moreover, since the peak or inactivating component of release flux (which results in an initial fast rise in $[Ca^{2+}]_i$) is systematically reduced by ClO_4^- at voltages near threshold, the determinations of Csernoch et al. (1987) may have overestimated Q_{th} by overlooking movements of reduced speed.

The ΔQ_{th} effect is remarkable for affecting what is by definition a parameter of coupling. Since Lüttgau et al. (1983) the effect of ClO_4^- on Ca release has been explained as secondary to its effect on charge movement: ClO_4^- shifts the mechanical threshold voltage because it shifts $Q(V)$. The fact that ClO_4^- reduces Q_{th} makes this explanation insufficient, as elaborated below.

The Mechanism of Action of Perchlorate

Pharmacological effects are usually attributed to specific binding to a discrete site on a target molecule. It is possible, however, that ClO_4^- is acting through a more physical mechanism that does not require selective binding.

Since Hofmeister (1888), who arranged some salts according to their protein precipitating effects (the lyotropic series), many have noted that the same or slightly altered sequences appear in a number of other effects. These so-called chaotropic or Hofmeister effects have been rationalized with the hypothesis that the Hofmeister salts or ions act by changing the structure of bulk water or of water at the interface (Creighton, 1984). It is hypothesized, with some experimental basis, that solutes at one extreme of the Hofmeister series increase the entropy of water surrounding nonpolar solutes, destroying the short-range hydrogen-bonded order (Hatefi and Hanstein, 1969; Von Hippel and Schleich, 1969). These are the chaotropes, like ClO_4^-, SCN^-, and I^-. At the other extreme, SO_4^{2-} and HPO_4^{2-} are termed kosmotropes. Through this fundamental property the effects of chaotropes are explained, including the solubilization of proteins and the dissociation of protein complexes into subunits, as both processes require an entropically unfavorable increase in the area of the protein–water interface, and are thus favored by the chaotropic action.

The chaotropic theory cannot explain some protein-dissociating effects that start at salt concentrations well under 100 mM (cf. below), since at 100 mM there is one solute ion every 550 molecules of water at 25°C. There are alternatives to the chaotropic theory that are not subject to the same criticism; for instance, the dissociation of a protein multimer may be due to preferential binding of the ions to the protomers rather than the multimer (Aune, Goldsmith, and Timasheff, 1971). The theory of preferential binding was shown by Sawyer and Puckridge (1973) to explain the dissociation of the octamer of β-lactoglobulin by NaSCN and other salts. It is interesting that the preferential binding theory leads to a similar order of potency of ions as the chaotropic theory, especially when the dissociation of protein multimers involves breaking of hydrogen bonds (as is the case for β-lactoglobulin; Sawyer and Puckridge, 1973).

The potency of the EC coupling effects of five anions (SO_4^{2-}, Br^-, NO_3^-, I^-, and SCN^-) is in general agreement with their ranking in the Hofmeister series (Delay, García, and Sánchez, 1990). Therefore, an explanation of the EC coupling effects of these anions could be based on their chaotropic effects on water. Such a chaotropic theory, however, is again untenable, as the effects of ClO_4^- on EC coupling start at 1

mM [ClO_4^-] (Fill and Best, 1990). Thus, rather than a change in the properties of water, a preferential binding to the EC coupling molecules is likely to underlie the effect.

Chromatographic experiments (Von Hippel, Peticolas, Schack, and Karlson, 1973) have shown that Hofmeister ions can bind to the amide dipole in peptides, with affinities that follow the lyotropic series. It is thus reasonable to hypothesize that ClO_4^- exerts its effects by binding to the EC coupling molecules. Possible locations of the ClO_4^- binding sites are considered next.

The Site of Perchlorate Action

Three possible binding sites will be considered. ClO_4^- may bind at the voltage sensor or at the release channel. Within the voltage sensor it may bind at a site accessible to the external solution (site I), to an intramembranous site, or to a site accessible from the myoplasm (site II). Sites on the release channel will be termed III.

Previous works point to the voltage sensor as the primary target: Lüttgau et al. (1983), Huang (1986, 1987), Csernoch et al. (1987), Delay et al. (1990), and Gyorke and Palade (1992) all found large effects of ClO_4^- on $Q(V)$. On skinned fibers Fill and Best (1990) showed that ClO_4^- increased the sensitivity to activation by ionic substitution without changing the sensitivity to activation by caffeine, which they interpreted as evidence of an effect on the sensor rather than the release channel. Stephenson (1989) likewise found potentiation of release by ionic substitution in skinned fibers and showed that ClO_4^- did not alter unstimulated ^{45}Ca efflux. All these results are in favor of sites I and II. The results of Fill and Best (1990) and Stephenson (1989) are in principle against III.

That ClO_4^- (Gomolla, Gottschalk, and Lüttgau, 1983; Csernoch et al., 1987) or SCN^- (Delay et al., 1990) have equal effects when administered internally or externally rules out possibility I and is consistent with intracellular or intramembranous sites (II or III).

That the τ_{off} of charge 1 is increased but that of charge 2 is not has two possible interpretations: either ClO_4^- binds to the voltage sensor in a state-dependent manner (not binding to its inactivated states) or ClO_4^- binds to the release channel and affects the voltage sensor allosterically, secondarily to its interaction with the release channel. The differential effect on charge 1 follows, simply because when charge 2 is generated (in the inactivated states) the voltage sensor does not control the release channel.

A site facing the myoplasm would require considerable permeability of the plasma and T membranes to the anion. The permeability to ClO_4^- is extremely low for artificial bilayers, but increases substantially in the presence of chloro-decane (Dilger, McLaughlin, McIntosh, and Simon, 1979) or in protein-rich mitochondrial microsomes (Berry, E., and P. Hinkle, cited in Dilger et al., 1979), in which the permeability to both ClO_4^- and SCN^- reaches a value of 2×10^{-6} cm/s. With this permeability a 10-mM gradient raises the concentration in a 100-μm-diam cylinder to ~1 mM in 1 s. Therefore, given the known permeability to the chaotropes, an intracellular site of action is not inconsistent with rapid onset and reversal of the effects. Moreover, the delay in reversal of the effects, found in the experiments

illustrated in Fig. 22, is also consistent with a molecule of limited permeability acting intracellularly.

A substantial permeability is also revealed by the recent demonstration that SCN^- collapses both the voltage and the H^+ gradient generated in proteoliposomes, through electrogenic Ca^{2+}/H^+ countertransport, by the SR Ca^{2+} pump (Yu, Carroll, Rigaud, and Inesi, 1993). SCN^- must cross the membrane in both charged and neutral (protonated) form to collapse the gradients. ClO_4^-, currently under study (Inesi, G., personal communication), probably does the same.

The fact that ClO_4^- reduces ΔQ_{th} indicates that the effect is not entirely reducible to a primary action on the voltage sensor. The primary effect includes a change in the coupling process. The new observation is consistent with binding sites on either molecule. However, if the site was on the sensor, ClO_4^- binding would have to increase its signaling ability. Likewise, if it bound to the release channel it would have to increase its propensity to opening.

The effects of ClO_4^- are very similar to those of R(+)CPP, an enantiomer of 2-(4-chlorophenoxy) carboxylic acid (Heiny et al., 1990). This enantiomer (but not the S(−)) increases the OFF time constant of intramembrane charge movement, shifts $\overline{V}$ to the left by ~8 mV, reduces the mechanical threshold, and increases contractility. Interestingly, the S(−) enantiomer is a Cl^- channel blocker and the R(+) compound increases Cl^- conductance. ClO_4^- and R(+)CPP are likely to act at the same EC coupling sites. These sites therefore are stereospecific and probably unrelated to the sites where both molecules (and the S(−)CPP) affect Cl conductance. Therefore the results on CPP agree with our observation that $\Delta\tau_{off}$ and the voltage shift have different requirements and suggest separate sites for EC coupling and Cl channel effects.

In this view, the $\Delta\overline{V}$ effect would be due, at least in part, to partition or binding of these anions to the T tubule membrane, and would not be related to the other EC coupling effects. Indeed, ClO_4^- and all Cl channel agonists and antagonists shift the voltage dependencies negatively, regardless of the EC coupling effect. Negative shifts were observed for both CPP enantiomers (Heiny et al., 1990), although the shift by S(−)CPP was not significant statistically, and for other Cl channel blockers (Bryant and Valle, 1981).

A primary effect of ClO_4^- on the voltage sensor may explain many of the observations: assume that there are two classes of mobile charge, say, Q_β and Q_γ, and that Q_β is either less effective in eliciting Ca release, or is unable to do so. Then, if ClO_4^- converted Q_β to Q_γ, Q_{th} would be reduced and $Q(V)$ would be made steeper. This explanation requires additional assumptions on the effect of ClO_4^-: the agonist should also make charge movement slower, but without changing its limiting rates at high voltage. Explanations like this one become less attractive in the next article, where it is shown that ClO_4^- increases the P_o of isolated release channels. Moreover, in the third article of this series we show that ClO_4^- changes the whole relationship between release flux and charge transferred in ways that cannot simply be explained by charge interconversion or shifts in $Q(V)$.

In summary, this discussion suggests that binding sites face the myoplasm. They may be on the sensor, but occupancy should then change the sensor's signaling function rather than just shift its voltage dependence. Or, they could be on the

release channel, but that would require an allosteric interaction with the sensor to explain the effects on charge movement. The second article of this series, in which the effects of ClO_4^- are explored on individual molecules of EC coupling reconstituted in bilayers, will show that ClO_4^- has major effects on the release channel but not on the DHP receptor when the molecules are separated. This favors sites of type III and an allosteric interaction between the molecules of EC coupling.

The Effects on Q_γ Require Ca Release

In every experiment carried out at low intracellular buffer concentration, ClO_4^- increased the steepness of the $Q(V)$ distribution, over twofold in some cases. When a hump component of charge movement was present at the ON, ClO_4^- made it greater and caused it to appear at lower test voltages (Fig. 15). In other experiments there was no visible hump in reference and an obvious one appeared in ClO_4^- (Fig. 5). A hump ON current and a steep voltage dependence are two characteristics by which Q_γ is defined (Hui and Chandler, 1990). According to both criteria ClO_4^- increased Q_γ. The magnitude of the increase could have been evaluated, for instance by fitting the sum of two Boltzmann functions to $Q(V)$ data (Hui and Chandler, 1990), but we felt that the quality of our data was not sufficient for such a fit.

There are at present two views regarding the nature of Q_γ (reviewed by Ríos and Pizarro, 1991); according to one of them (Huang, 1989; Hui and Chandler, 1991) Q_γ and Q_β result from the movement of two chemically different voltage sensors (γ and β), the γ sensor moving more slowly and having a much greater valence. In the other view (Csernoch et al., 1991; García et al., 1991; Pizarro et al., 1991; Szücs, Csernoch, Magyar, and Kovács, 1991*a*) there is nothing intrinsically different between the sensors and Q_γ moves as a consequence of an increase in local potential due to a local increase in $[Ca^{2+}]_i$. These two views must be accompanied of different interpretations of the ClO_4^- effects: in the γ sensor hypothesis, ClO_4^- must be a specific agonist of Q_γ which augments the amount, or $Q_{\gamma max}$, making new sensors available to generate Q_γ (and increasing the overall steepness of the voltage distribution). In the Ca binding hypothesis, the increase in Q_γ could be related to the lowering of Q_{th}; by causing release at lower levels of charge, ClO_4^- brings the Ca binding to play when less charge has moved, and more is available to be moved by the positive feedback of Ca acting on the sensors. A quantitative model shows that this is the case for a simple class of potentiating mechanisms (Pizarro, Csernoch, and Ríos, 1991*a*).

Two additional results in this study help to decide between the above possibilities. One is that ClO_4^- does not increase the steepness of $Q(V)$ (or increases it only slightly) after the depletion caused by repeated pulsing in BAPTA, EGTA, or both. It does not really matter whether the loss of the ΔK effect of ClO_4^- was the result of depletion or buffering, which prevents the local increase in $[Ca^{2+}]_i$. In the Ca binding model both should contribute to the elimination of ΔK. A purely pharmacological effect of the buffers that eliminates Q_γ cannot be ruled out, but is unlikely since the effect was also observed in experiments with very high EGTA and the buffers were not deleterious in any other way that we could see. Moreover, the simple presence of buffers was not sufficient to eliminate humps and the ΔK effect, but the combination of the buffer and frequent pulsing was necessary. Thus, the combined effects of ClO_4^- with buffers and pulsing are consistent with the Ca binding hypothesis.

The second result relevant to this issue is the constancy of total mobile charge Q_{max} in spite of large changes in steepness, revealing large changes in Q_γ. If, as we must conclude, Q_γ increased substantially, then the total Q_β must have decreased by the same amount. Therefore, in the γ sensor hypothesis ClO_4^- must have equal and opposite effects on both classes of sensors.

In the Ca binding hypothesis, on the other hand, the constancy of Q_{max} is an inevitable consequence of assuming a single population of sensors, which may move as Q_β or Q_γ, depending on the voltage and how much the local $[Ca^{2+}]_i$ increases, but end up contributing to Q_{max} as the voltage is sufficiently increased. In the Ca binding model, the difference between Q_β and Q_γ is not fundamental; in other words, Q_γ and Q_β are not thermodynamic functions of state (V being the state variable), but also depend on the path taken to a given V. This implies that their rates of change, I_γ and I_β, are not exact differentials. Thus, in the Ca binding hypothesis it is more consistent to refer to I_β and I_γ rather than to their integrals Q_β and Q_γ, as the latter depend on the integration path.

Based on the observation that the steepness of the voltage distribution of Q_γ is greater than that of Q_β by a factor close to 4, Hui and Chandler (1990) have suggested that Q_β could result from transitions in individual protein molecules, while Q_γ would arise in rearrangements of the voltage sensors in groups of four. This suggestion bridges in some ways the two alternatives discussed before: Q_γ and Q_β would no longer be fundamentally different species but the same protein in different states of interaction or cooperativity. This proposal would naturally account for the conservation of Q_{max} observed in this study. The proposal, however, does not explain the existence of an inward phase of charge movement during depolarizing pulses, which was reported by Pizarro et al. (1991*b*) and then questioned by Hui and Chen (1991). The observation of an inward phase in I_γ was recently extended by Shirokova, González, and Ríos (1993).

We are grateful to Dr. Gonzalo Pizarro and Dr. Ismael Uribe for allowing us to use the results of their earlier experiments in this paper, and to Dr. Natalia Shirokova for carrying out additional studies on the stability of SR Ca content in reference solutions. We thank Dr. Giuseppe Inesi for kindly sharing unpublished evidence of the permeability of liposomes to SCN^- and ClO_4^-.

This work was supported by the United States Public Health Service, by National Institute of Arthritis and Musculoskeletal and Skin Diseases grant AR-32808, and by a research grant from the Muscular Dystrophy Association of America.

Original version received 29 July 1992 and accepted version received 20 May 1993.

REFERENCES

Aune, K. C., L. C. Goldsmith, and S. N. Timasheff. 1971. Dimerization of α-chymotrypsin II. Ionic strength and temperature dependence. *Biochemistry.* 10:1617–1622.

Bretag, A. H. 1987. Muscle chloride channels. *Physiological Reviews.* 67:618–717.

Brum, G., and E. Ríos. 1987. Intramembrane charge movement in frog skeletal muscle fibres: properties of charge 2. *Journal of Physiology.* 387:489–517.

Brum, G., E. Ríos, and E. Stefani. 1988. Effects of extracellular calcium on the calcium movements of excitation contraction coupling in skeletal muscle fibers. (With an appendix by G. Brum, E. Ríos, and M. F. Schneider.) *Journal of Physiology.* 398:441–473.

Bryant, S. H., and R. Valle. 1981. Action of antrhracene-9-carboxylic acid on the mechanical response of single skeletal muscle fibers. *Biophysical Journal.* 33:153*a*. (Abstr.)

Caputo, C., and P. Bolaños. 1989. Effects of D-600 on intramembrane charge movement of polarized and depolarized frog muscle fibers. *Journal of General Physiology.* 94:43–64.

Chandler, W. K., and C. S. Hui. 1990. Membrane capacitance in frog cut twitch fibers mounted in a double Vaseline-gap chamber. *Journal of General Physiology.* 96:225–256.

Chandler, W. K., R. F. Rakowski, and M. F. Schneider. 1976. Effects of glycerol treatment and maintained depolarization on charge movement in skeletal muscle. *Journal of Physiology.* 254:285–316.

Cleland, W. W. 1967. The statistical analysis of enzyme kinetic data. *Advances in Enzymology and Related Areas of Molecular Biology.* 29:1–32.

Collins, K. D., and M. W. Washabaugh. 1985. The Hofmeister effect and the behaviour of water at interfaces. *Quarterly Review of Biophysics.* 18:323–422.

Creighton, T. E. 1984. Proteins. Structures and Molecular Properties. W. H. Freeman and Co., New York. 134–158.

Csernoch, L., L. Kovacs, and G. Szucs. 1987. Perchlorate and the relationship between charge movement and contractile activation in frog skeletal muscle fibres. *Journal of Physiology.* 390:213–227.

Csernoch, L., G. Pizarro, I. Uribe, M. Rodríguez, and E. Ríos. 1991. Interfering with calcium release suppresses Q_γ, the delayed component of intramembrane charge movement in skeletal muscle. *Journal of General Physiology.* 97:845–884.

Delay, M., D. E. García, and J. A. Sánchez. 1990. The effects of lyotropic anions on charge movement, calcium currents and calcium signals in frog skeletal muscle fibres. *Journal of Physiology.* 425:449–469.

Dilger, J. P., S. G. McLaughlin, T. J. McIntosh, and S. A. Simon. 1979. The dielectric constant of phospholipid bilayers and the permeability of membranes to ions. *Science.* 206:1196–1198.

Fill, M. D., and P. M. Best. 1990. Effect of perchlorate on calcium release in skinned fibres stimulated by ionic substitution and caffeine. *Pflügers Archiv.* 415:688–692.

Francini, F., and E. Stefani. 1989. Decay of the slow calcium current in twitch muscle fibers of the frog is influenced by intracellular EGTA. *Journal of General Physiology.* 94:953–969.

García, J., G. Pizarro, E. Ríos, and E. Stefani. 1991. Effect of the calcium buffer EGTA on the "hump" component of charge movement in skeletal muscle. *Journal of General Physiology.* 97:885–896.

Gomolla, M., G. Gottschalk, and H. C. Lüttgau. 1983. Perchlorate-induced alterations in electrical and mechanical parameters of frog skeletal muscle fibres. *Journal of Physiology.* 343:197–214.

Gyorke, S., and P. Palade. 1992. Effects of perchlorate on excitation-contraction coupling in frog and crayfish skeletal muscle. *Journal of Physiology.* 456:443–451.

Harafuji, H., and Y. Ogawa. 1980. Reexamination of the apparent binding constants of ethyleneglycol bis(β-aminoethyl-ether)-*N,N,N′,N′*-tetraacetic acid with calcium around neutral pH. *Journal of Biochemistry.* 87:1305–1312.

Hatefi, Y., and W. G. Hanstein. 1969. Solubilization of particulate proteins and nonelectrolytes by chaotropic agents. *Proceedings of the National Academy of Sciences, USA.* 62:1129–1136.

Heiny, J., and D. Jong. 1990. A non-linear electrostatic potential change from the T-system of skeletal muscle detected under passive recording conditions using potentiometric dyes. *Journal of General Physiology.* 95:147–176.

Heiny, J., D. Jong, S. H. Bryant, D. Conte-Camerino, and V. Tortorella. 1990. Enantiomeric effects on charge movement and mechanical threshold in frog skeletal muscle by a chiral phenoxy carboxylic acid. *Biophysical Journal.* 57:147–152.

Hodgkin, A. L., and P. Horowicz. 1960*a*. The effect of sudden changes in ionic concentration on the membrane potential of single muscle fibers. *Journal of Physiology*. 153:370–385.

Hodgkin, A. L., and P. Horowicz. 1960*b*. Potassium contractures in single muscle fibers. *Journal of Physiology*. 153:386–403.

Hofmeister, F. 1888. On the understanding of the effect of salts. Second report. On regularities in the precipitatin effect of salts and their relationship to their physiological behavior. *Naunyn-Schmiedebergs Archiv für Experimentelle Pathologie und Pharmakologie*. 24:247–260.

Huang, C. L. H. 1986. The differential effects of twitch potentiators on charge movements in frog skeletal muscle. *Journal of Physiology*. 380:17–33.

Huang, C. L. H. 1987. 'Off' tails of intramembrane charge movements in frog skeletal muscle in perchlorate containing solutions. *Journal of Physiology*. 384:491–510.

Huang, C. L. H. 1989. Intramembrane charge movements in skeletal muscle. *Physiological Reviews*. 68:1197–1247.

Hui, C. S., and W. K. Chandler. 1990. Intramembranous charge movement in frog cut twitch fibers mounted in a double Vaseline-gap chamber. *Journal of General Physiology*. 96:257–298.

Hui, C. S., and W. K. Chandler. 1991. Q_β and Q_γ components of intramembranous charge movement in frog cut twitch fibers. *Journal of General Physiology*. 98:429–464.

Hui, C. S., and W. Chen. 1991. Does the hump charge movement component have a negative phase? *Biophysical Journal*. 59:543*a*. (Abstr.)

Irving, M., J. Maylie, N. L. Sizto, and W. K. Chandler. 1987. Intrinsic optical and passive electrical properties of cut frog twitch fibers. *Journal of General Physiology*. 89:1–41.

Kovacs, L., E. Ríos, and M. F. Schneider. 1979. Calcium transients and intramembrane charge movement in skeletal muscle fibers. *Nature*. 279:391–396.

Lüttgau, H. C., G. Gottschalk, L. Kovacs, and M. Fuxreiter. 1983. How perchlorate improves excitation-contraction coupling in skeletal muscle fibres. *Biophysical Journal*. 43:247–249.

Martell, A. E., and R. M. Smith. 1974. Critical Stability Constants. Vol. 1. Plenum Publishing Corp., New York, 727 pp.

Melzer, W., E. Ríos, and M. F. Schneider. 1984. Time course of calcium release and removal in skeletal muscle fibers. *Biophysical Journal*. 45:637–641.

Melzer, W., E. Ríos, and M. F. Schneider. 1987. A general procedure for determining calcium release in skeletal muscle fibers. *Biophysical Journal*. 51:849–864.

Nabauer, M., G. Callewaert, L. Cleemann, and M. Morad. 1989. Regulation of calcium release is gated by calcium current, not gating charge, in cardiac myocytes. *Science*. 244:800–803.

Pizarro, G., L. Csernoch, and E. Ríos, 1991*a*. Modeling Q_γ and positive feedback in EC coupling of skeletal muscle. *Biophysical Journal*. 59:67*a*. (Abstr.)

Pizarro, G., L. Csernoch, I. Uribe, M. Rodríguez, and E. Ríos. 1991*b*. The relationship between Q_γ and Ca release from the sarcoplasmic reticulum in skeletal muscle. *Journal of General Physiology*. 97:913–947.

Provencher, S. W. 1976. Fourier method for the analysis of exponential decay curves. *Biophysical Journal*. 16:27–41.

Ríos, E., J. Ma, and A. González. 1991. The mechanical model of excitation-contraction coupling in skeletal muscle. *Journal of Muscle Research an Cell Motility*. 12:127–135.

Ríos, E., and G. Pizarro. 1991. The voltage sensor of excitation-contraction coupling in skeletal muscle. *Physiological Reviews*. 71:849–908.

Ríos, E., G. Pizarro, and G. Brum. 1989. A four gap voltage clamp improves measurements of EC coupling events in frog skeletal muscle. *Biophysical Journal*. 55:237*a*. (Abstr.)

Sawyer, W. H., and J. Puckridge. 1973. The dissociation of proteins by chaotropic salts. *Journal of Biological Chemistry*. 248:8429–8433.

Scarborough, J. B. 1966. Numerical Mathematical Analysis. 6th ed. Johns Hopkins University Press, Baltimore. 540 pp.

Schneider, M. F., and W. K. Chandler. 1973. Voltage dependent charge movement in skeletal muscle: a possible step in excitation-contraction coupling. *Nature.* 242:244–246.

Schneider, M. F., E. Ríos, and W. Melzer. 1987*a*. Determining the rate of calcium release from the sarcoplasmic reticulum in muscle fibers. *Biophysical Journal.* 51:1005–1007.

Schneider, M. F., B. J. Simon, and G. Szűcs. 1987*b*. Depletion of calcium from the sarcoplasmic reticulum during calcium release in frog skeletal muscle. *Journal of Physiology.* 392:167–192.

Shirokova, N., A. González, and E. Ríos. 1993. Three phases in I_γ, the hump component of charge movement in skeletal muscle. *Biophysical Journal.* 64:A240. (Abstr.)

Smith, P. D., G. W. Liesegang, R. L. Berger, G. Czierlinski, and R. J. Pololsky. 1984. A stopped flow investigation of calcium ion binding by ethylene glycol bis(β-aminoethylether)-*N,N'*-tetracetic acid. *Analytical Biochemistry.* 143:188–195.

Stephenson, D. G. 1987. Calcium release from the sarcoplasmic reticulum. *Biophysical Journal.* 51:1009–1010.

Stephenson, E. W. 1989. Excitation of skinned muscle fibers by imposed ion gradients. IV. Effects of stretch and perchlorate ion. *Journal of General Physiology.* 93:173–192.

Szücs, G., L. Csernoch, J. Magyar, and L. Kovács. 1991*a*. Contraction threshold and the "hump" component of charge movement in frog skeletal muscle. *Journal of General Physiology.* 97:897–911.

Szücs, G., Z. Papp, L. Csernoch, and L. Kovács. 1991*b*. Kinetic properties of intramembrane charge movement under depolarized conditions in frog skeletal muscle fibers. *Journal of General Physiology.* 98:365–378.

Von Hippel, P. H., V. Peticolas, L. Schack, and L. Karlson. 1973. Model studies on the effects of neutral salts on the conformational stability of biological macromolecules. I. Ion binding to polyacrylamide and polystyrene columns. *Biochemistry.* 12:1256–1264.

Von Hippel, P. H., and T. Schleich. 1969. Structure and Stability of Biological Macromolecules. S. M. Timasheff and G. D. Fasman, editors. Marcel Dekker, Inc., New York. 417–574.

Yu, X., S. Carroll, J.-L. Rigaud, and G. Inesi. 1993. H^+ countertransport and electrogenicity of the sarcoplasmic reticulum Ca^{2+} pump in reconstituted proteoliposomes. *Biophysical Journal.* 1232–1242.